



Manuscript 1469

## Recovery of magnesium sulfate and calcium sulfate from zinc flotation tailing

Author(s) ORCID Identifier:

Raquel Húngaro Costa: (D) 0000-0002-3314-9018 Jonathan Tenório Vinhal: (D) 0000-0002-4391-2443

Tatiana Scarazzato: (D) 0000-0002-9526-1937

Denise Crocce Romano Espinosa: Denise Crocce Romano Espinosa:

Follow this and additional works at: https://jsm.gig.eu/journal-of-sustainable-mining

Part of the Explosives Engineering Commons, Oil, Gas, and Energy Commons, and the Sustainability Commons

### Recovery of magnesium sulfate and calcium sulfate from zinc flotation tailing

#### Abstract

Resource recovery is a process that has been used to obtain products from industrial waste. Mining tailings can be used as an alternative through ore beneficiation to create by-products for this type of waste. The work herein investigated the recovery of two products from a real tailing generated in the Zn beneficiation route in the flotation step. A non-magnetic fraction was submitted to a hydrometallurgical route to produce MgSO<sub>4</sub> and CaSO<sub>4</sub>. Thermodynamic simulations using *FactSage* software were performed to evaluate the optimal leaching conditions varying the S:L ratio, the sulfuric acid concentration, and temperature. The best modeled conditions for pure dolomite were established in 1.2 mol×L<sup>-1</sup> H<sub>2</sub>SO<sub>4</sub>, S:L ratio 1:10, at room temperature, showing 100% Mg extraction. The simulation with the real composition showed 100% Mg extraction using 1.0 mol×L<sup>-1</sup> H<sub>2</sub>SO<sub>4</sub>, S:L ratio 1:10, at room temperature. Experimental leaching tests led to Mg and Ca extraction yields of 72% ±5 and 2%, respectively, obtained at 50°C in 35 min. The cementation step resulted in 92.3% of Cd removal from the leach liquor with Zn:Cd ratio of 100:1 in 5 min at 25°C. The obtained by-products were CaSO<sub>4</sub> and solubilized MgSO<sub>4</sub>. Both are potentially usable for agriculture purposes, being magnesium sulfate a secondary macronutrient as fertilizer, and CaSO<sub>4</sub> as a soil conditioner.

#### **Keywords**

Resource recovery; Hydrometallurgy; Mining tailing; Magnesium sulfate; Calcium sulfate.

#### **Creative Commons License**



This work is licensed under a Creative Commons Attribution-Noncommercial-No Derivative Works 4.0 License.

# Recovery of magnesium sulfate and calcium sulfate from zinc flotation tailing

Raquel H. Costa\*, Jonathan T. Vinhal, Tatiana Scarazzato, Denise C.R. Espinosa

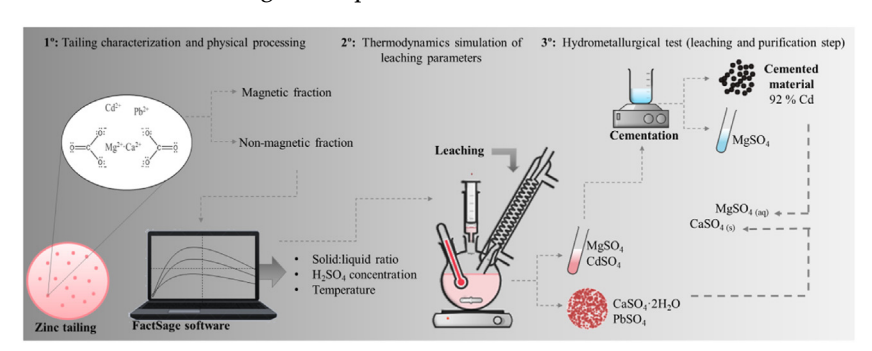
University of São Paulo, Polytechnic School, Chemical Engineering Department, Rua do Lago, 250, Cidade Universitária, Butantã, 05508-030, São Paulo, Brazil

#### Abstract

Resource recovery is a process that has been used to obtain products from industrial waste. Mining tailings can be used as an alternative through ore beneficiation to create by-products for this type of waste. The work herein investigated the recovery of two products from a real tailing generated in the Zn beneficiation route in the flotation step. A non-magnetic fraction was submitted to a hydrometallurgical route to produce MgSO<sub>4</sub> and CaSO<sub>4</sub>. Thermodynamic simulations using *FactSage* software were performed to evaluate the optimal leaching conditions varying the S:L ratio, the sulfuric acid concentration, and temperature. The best modeled conditions for pure dolomite were established in 1.2 mol·L<sup>-1</sup> H<sub>2</sub>SO<sub>4</sub>, S:L ratio 1:10, at room temperature, showing 100% Mg extraction. The simulation with the real composition showed 100% Mg extraction using 1.0 mol·L<sup>-1</sup> H<sub>2</sub>SO<sub>4</sub>, S:L ratio 1:10, at room temperature. Experimental leaching tests led to Mg and Ca extraction yields of 72% ±5 and 2%, respectively, obtained at 50°C in 35 min. The cementation step resulted in 92.3% of Cd removal from the leach liquor with Zn:Cd ratio of 100:1 in 5 min at 25°C. The obtained by-products were CaSO<sub>4</sub> and solubilized MgSO<sub>4</sub>. Both are potentially usable for agriculture purposes, being magnesium sulfate a secondary macronutrient as fertilizer, and CaSO<sub>4</sub> as a soil conditioner.

#### Highlights

- Waste minimization proposal for a mining tailing containing 90 wt.% dolomite.
- Recovery of two by-products CaSO<sub>4</sub> and MgSO<sub>4</sub>.
- Simulations proved to be a good basis for selecting leaching parameters.
- Cementation removed 92% Cd from Mg-rich liquor.



Keywords: Resource recovery, Hydrometallurgy, Mining tailing, Magnesium sulfate, Calcium sulfate

#### 1. Introduction

T he demand for metals is intrinsic to society's development, especially due to the new

technologies currently present. There is constant population growth, and the demand for raw materials is also larger to supply their needs. To obtain these minerals as products (metallic or oxides) to be

Received 26 February 2024; revised 8 November 2024; accepted 10 November 2024. Available online 1 October 2025

\* Corresponding author.

E-mail address: rhungarocosta@gmail.com (R.H. Costa).

applied in technologies or in general use, techniques known as extractive metallurgy are used [1]. Zinc is the third most common metal of the nonferrous group — aluminum and copper are above it. The galvanizing supply industries are dependent on the extraction and beneficiation of Zn due to a common process of coating to prevent metals from corrosion - e.g., mostly steel or iron. The method used for obtaining Zn is known as hydrometallurgy and pyrometallurgy. Sulfides, oxides, and silicates are the composition of Zn ores [2]. To obtain a Zn concentrate, the flotation step is used in the beneficiation process. Usually, in flotation, a gangue is produced, which may be a compound of dolomite, goethite, quartz, kaolinite, calcite, barite, and feldspar [3-5]. The gangue composition may be diversified due to the location and geologic environment [6]. Also, elements considered toxic metals, such as Pb and Cd can be found in Zn tailing. However, studying strategies and alternatives to reduce or even eliminate these elements is fundamental to obtaining a by-product from Zn tailing [7–9].

Mineral processing industries bring consequences such as the volume of waste generated and the volume of processed materials. For example, according to United States Geological Survey, Zn beneficiation has a world production estimated at 13.8 million tons [10]. In mineral processing, a problem faced by the companies is the final destination, followed by controlling the tailing generation. Examples of recycling material alternatives are important: in the United States, in 2022, it was estimated that 60% of refined zinc was recovered from secondary materials in primary and secondary smelters [11].

Some impacts occur in mining fields, while some examples are deforestation, road construction (to access the whole infrastructure to the mine), drilling, and site exploration - those represent an entire chain of impacts. Some other given examples are stockpiling of waste and tailing dams; excessive use of water for many purposes; natural habitat disturbances; in some cases, cultural heritage; noise pollution; accidental or deliberated release of untreated solid/liquid/gaseous contaminants into the ecosystem [12]. Therefore, methods and techniques that aim to reduce impacts and achieve a better use of resources, focusing on minimizing exploitation, are one of the keys to pursue sustainable development [13,14].

Alternatives were shown according to previous studies that focus on reusing or even recycling tailings from metal beneficiation in mining fields [8,9,15,16]. Some options for materials acquired from the recycling mining tailing are focused on

obtaining by-products in agroforestry, building materials, coatings, resin products, glass, and ceramics. Materials stored in landfills can be used as secondary material with a new purpose. These purposes are, for example, to return as clay-rich to improve sandy soils. Also, they may be used as fertilizers in agriculture or in the construction industry [12]. The reuse of biomass after a thermochemical treatment/incineration/wet extraction was applied as N, P, K, and Mg macronutrient fertilizer in a study reported by Chojnacka et al., (2019) [17]. Techniques such as cementation are essential for the purification step to reuse tailing aimed at obtaining by-products [1,18]. Magnesium sulfate is known as a fertilizer in agriculture, and it is also considered a secondary macronutrient along with C, H, O, N, P, K, Ca, and S. Meanwhile, calcium sulfate is known as a soil conditioner. Thus, a natural source for these elements, Mg and Ca, is dolomitic limestone - a gangue from Zn tailing [19].

Furthermore, magnesium is also considered a critical element, according to Perez et al. (2019) [20], due to its economic importance and supply risk. Critical raw materials are obtained from natural source exhaustion and are defined as difficult to replace. Besides that, their ores are found in low concentration, and there is a risk of abruption supply disruption [20]. Alternatives from tailings deemed to be non-explorable may be a solution to recover such elements and acquire by-products using hydrometallurgical routes. Hence, eliminating or reducing toxic metals from tailings focusing on by-products also contributes to reducing the exploitation of new resources coming upon to sustainability concepts [20–25].

Thus, focusing on recovering Mg and Ca as sulfates from dolomite (gangue material in Zn tailing) was investigated in this work. The aim was to obtain a potential raw material (by-product) as fertilizers and soil conditioners, also to perform a preliminary study to remove toxic metals from these by-products, which was preliminary investigated, being an alternative for mining tailings.

#### 2. Materials and methods

#### 2.1. Composition of the tailing

A material from a beneficiation plant located in Minas Gerais, Brazil, was obtained to be investigated. This material was a tailing acquired from the Zn ore (willemite) from the flotation step. In a previous study, the characterization and physical processing of the tailing was presented [26–29]. According to the prior results, the composition

of the dolomite-rich fraction (non-magnetic material using a rougher cleaner route), as shown in Figure 1, was characterized by the main components of 0.34% Al, 21.62% Ca, 0.04% Cd, 2.70% Fe, 11.91% Mg, 0.08% Mn, 0.21% Pb, 1.37% Si and 1.73% Zn. Dolomite was the predominant mineral in the non-magnetic fraction with 90.3 wt.%. This work aimed to investigate a hydrometallurgical route to produce MgSO<sub>4</sub> and CaSO<sub>4</sub> from the nonmagnetic fraction aforementioned. The leaching parameters were supported by thermodynamics simulations, as detailed in item 2.2. Also, a mass balance was proposed, estimating the mass of the main by-products, which were MgSO<sub>4</sub>·7H<sub>2</sub>O and CaSO<sub>4</sub> produced from a pre-fixed amount of tailing. The suggested route is described in Figure 1.

#### 2.2. Thermodynamic simulation of leaching parameters

The thermodynamic simulation software FactSage was initially developed for pyrometallurgy, and it has been constantly improved for several other applications, such as hydrometallurgy and electrometallurgy. The software contains databases, which allow one to evaluate the thermochemistry of the reactions involved in the process. The thermodynamic study in hydrometallurgy is based on chemical equilibrium. Therefore, calculations are

performed based on thermodynamic models for each phase, providing species and phase diagrams for aqueous/solid/gaseous compounds for pure substances or multicomponent systems. All thermodynamic and phase equilibrium data is evaluated for a given system that simultaneously obtains one set of model equations for the Gibbs energies as functions of temperature and composition are simulated [30,31].

The leaching parameters for simulation were performed with the aid of FactSage 7.2 Equilib module software, and the FactPS, FTmisc, and FToxid databases were established. Thus, aiming to establish the optimal leaching conditions with temperature, solid:liquid ratio, and leaching agent (H<sub>2</sub>SO<sub>4</sub>) concentration to produce MgSO<sub>4</sub> from dolomite was evaluated, according to Equation (1).

$$CaMg(CO3)2 + 2H2SO4 \rightarrow MgSO4 + CaSO4 \cdot 2H2O \( \psi + 2CO2 \) \( \psi \) (1)$$

The input data were provided considering 100 g of pure dolomite [CaMg(CO<sub>3</sub>)<sub>2</sub>]. Nevertheless, a fraction of impurities could be found in the tailing. Due to that, the simulation was carried out in two steps: Step one) conditions using pure dolomite (100 g). Step two) conditions using dolomite (90.3 g) with impurities (9.7 g) based on the characterized Zn tailing material.

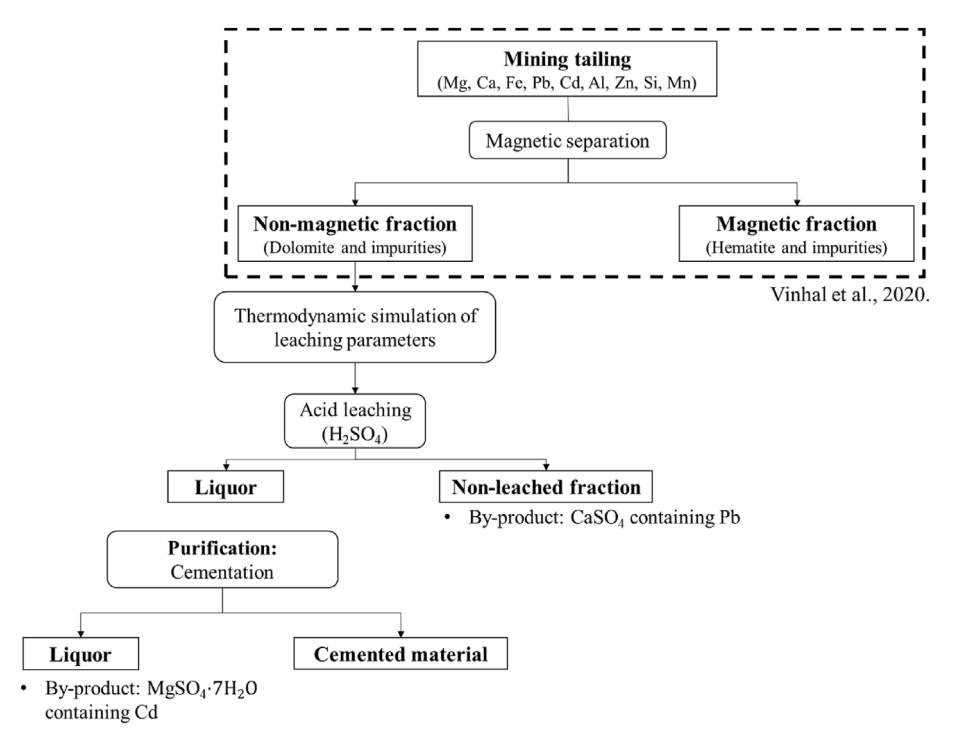


Fig. 1. Flowchart diagram showing the proposed process for the recovery of Mg and Ca by-products from Zn tailing. Cited reference as Vinhal et al., 2020 [26].

For step one, the initial input data were selected as follows:

- Temperature: from 25°C to 90°C, at 5°C intervals;
- Solid:liquid ratio: 1:5 and 1:10;
- $H_2SO_4$  concentration: 0.5 mol·L<sup>-1</sup>, 1.0 mol·L<sup>-1</sup> and 2.0 mol·L<sup>-1</sup>.

After an initial screening of the thermodynamic simulations, another set of simulations was performed (closer to the optimal conditions), considering the following parameters:

- Temperature: from 25°C, 60°C and 90°C;
- Solid:liquid ratio: 1:4, 1:5, 1:6, 1:7, 1:8, 1:9, 1:10;
- $H_2SO_4$  concentration: 1.0 mol·L<sup>-1</sup>, 1.2 mol·L<sup>-1</sup>, 1.4 mol·L<sup>-1</sup>, 1.6 mol·L<sup>-1</sup>, 1.8 mol·L<sup>-1</sup> and 2.0 mol·L<sup>-1</sup>.

For step two, a simulation considering the real Zn tailing composition was carried out to evaluate the presence of impurities. The initial input data were selected using the following parameters:

- Temperature: from 25°C to 90°C, at 5°C intervals;
- Solid:liquid ratio: 1:10;
- $H_2SO_4$  concentration: 0.5 mol·L<sup>-1</sup>, 1.0 mol·L<sup>-1</sup> and 2.0 mol·L<sup>-1</sup>.

The focus on the simulation with pure dolomite was to evaluate the yield of Mg and Ca leaching. Simulation data from Zn tailing was evaluated to determine the yield of Mg, Ca, Pb, Cd, Zn, Al, and Fe extraction to be compared with the results of pure dolomite. The results with the highest predicted MgSO<sub>4</sub> formation in the simulation were chosen as optimal conditions to conduct the experimental leaching tests.

#### 2.3. Acidic leaching

To compare the simulation results, the leaching tests were carried out. The experimental tests evaluated different temperatures (25, 50, 75, and 90°C) under constant magnetic stirring. The leaching agent was a  $1.2 \text{ mol} \cdot \text{L}^{-1} \text{ H}_2 \text{SO}_4$  solution — as indicated by the simulation — while the reaction time was set to 180 min. The volume of the leaching solution was 0.5 L, and the mass of Zn tailing was 50 g.

The assembly consisted of a 1 L five-neck glass reactor placed on a heating and stirring plate. A condenser was connected to the reactor and coupled to a thermostatic bath. The temperature inside the reactor was monitored at 5-min intervals

with a thermometer placed in one neck of the reactor. Also, 2 mL samples were collected at a fixed time interval (5, 10, 20, 30 min) with the aid of a hydrophobic PTFE-25 mm  $\times$  0.45  $\mu$ m syringe filter.

Leaching tests were also carried out to assess the optimal concentration of  $\rm H_2SO_4$  by varying it in 0.8–1.0–1.2–1.5–2.0 mol·L<sup>-1</sup> at 50°C and fixing the reaction time in 35 min (all in duplicates). The tests were carried out in 0.25 L Erlenmeyer flasks under constant magnetic stirring, and the temperature was measured continuously every 5 min. The initial conditions in mass (tailing weight) and volume (leaching solution) were 10 g and 0.1 L, respectively, for all tests.

At the end of each test, the solution was submitted to a vacuum filtration system equipped with a quantitative paper filter (2 and 6  $\mu$ m) — obtaining the leach liquor. Then, a non-leached fraction was obtained and digested according to the procedure described in item 2.5.3. Both leach liquor and the non-leached fraction were forwarded to chemical analyses, as described in item 2.5.

#### 2.4. Cementation post-treatment

To remove reminiscent impurities from the leach liquor, especially Cd, a purification step was evaluated. First, a synthetic solution was studied to assess the behavior of Cd and Mg. Subsequently, tests were executed with real leach liquor.

The synthetic solution was prepared by dissolving MgSO<sub>4</sub>·7H<sub>2</sub>O and Cd(NO<sub>3</sub>)<sub>2</sub>·4H<sub>2</sub>O salts in a 1.2 mol·L<sup>-1</sup> H<sub>2</sub>SO<sub>4</sub> solution media. Then, Zn powder was added as a cementation agent with different Zn:Cd ratios (100:1, 50:1, 10:1, 5:1, 2.5:1 and 1:1) considering the Cd weight in grams. In this experiment, a magnetic stirrer was used at 600-800 rpm. Also, the temperature and time were fixed at 25°C and 20 min, respectively. The time effect in Cd cementation was evaluated through chemical analysis by atomic absorption spectroscopy (AAS) (see item 2.5) of 0.1 mL aliquots taken every 5 min from 1 to 50 min. The solution acquired was filtered after the fixed time in a filter paper. The non-leached fraction was characterized using Scanning electron microscopy/energy dispersive X-ray spectroscopy (SEM/EDS), described in item 2.5.

#### 2.5. Chemical analysis

The leaching (leach liquor and non-leached fraction) and cementation samples were analyzed with the following pieces of equipment: X-ray diffraction (XRD) and scanning electron microscopy paired with dispersive energy spectroscopy (SEM/EDS). Only solid materials were characterized in XRD and

SEM-EDS, in this case, the non-leached fraction and cemented particles. In contrast, the leach liquor was analyzed by the following analyses: ion chromatography (IC), atomic absorption spectroscopy (AAS), and inductively coupled plasma optical emission spectrometry (ICP-OES) for the quantification of Mg, Ca, Pb, Cd, Fe, Zn, Al, and Mn.

The non-magnetic fraction and non-leached fraction, when analyzed by ICP-OES, were submitted to a digestion step to then achieve a sample that is allowed to characterize the material in a liquid form.

#### 2.5.1. X-ray diffraction (XRD)

To evaluate the predominant phases of the non-leached fraction, X-ray diffraction was used. The equipment used was a Rigaku Miniflex 300 diffractometer, configured from 3° to 100° with 0.02 steps at 1.5°/min speed in step mode, scanning the non-leached fraction samples. To perform the samples' comminution into the most satisfactory particle sample (holder compacting), an agate mortar was used.

## 2.5.2. Scanning electron microscopy and dispersive energy spectroscopy (SEM-EDS)

To analyze the particle structure, scanning electron microscopy was performed using a Phenon ProX microscope coupled to an EDS instrument to identify and analyze semi-quantitatively the elements.

The equipment used for the SEM/EDS analyses was conducted in a Phenom Pro X benchtop microscope with an accelerating voltage of 15 kV and a back scattered electron detector (BSE). The SEM analyses with focused ions beams (FBI) were performed in a Quanta FEG (Field Emission Gun) from FEI Company with an accelerating voltage of 30 kV and a current of 29.6 pA for FIB images. Dispersive spectroscopy (EDS) was used to qualitatively characterize the samples.

## 2.5.3. Inductively coupled plasma optical emission spectrometry (ICP-OES)

Both leach liquor and non-leached fractions were performed for quantitative characterization of the elements by ICP-OES. The non-leached fraction was analyzed after microwave digestion using a CEM Corporation Modelo Mars 6 microwave instrument. The digestion was carried out by weighing 0.25 g of the solid sample and mixing different acids: 2 mL HF, 3 mL HNO<sub>3</sub>, and 5 mL HCl. The digestion was fixed in two stages: 1400–1600 W, ramp time for 5–10 min (first stage), holding time was for 15–35 min (second stage), the temperature at 160°C (first stage) to 210°C (second stage), and a Temp-Guard of 260°C. To neutralize the samples after

their digestion using the CEM microwave due to HF acid,  $20 \text{ mL H}_3\text{BO}_3$  was used (10 mL or 0.45 g was added for each 1 mL of HF). The samples digested were filtered and diluted in a solution of 25 or 50 mL. This procedure was fixed in one stage: 900-1500 W, ramp time for 15 min, holding time for 15 min, and a TempGuard of  $170^{\circ}\text{C}$ .

The quantitative chemical analyses for Ca, Cd, Fe, Pb, Al, Mn, and Zn were carried out by ICP-OES instrument (Agilent 710 Spectrometer) under the following conditions: plasmas flow 15.0  $L \cdot min^{-1}$ ; auxiliary Argon flow 1.50  $L \cdot min^{-1}$  and nebulizer pressure of 200 kPa.

#### 2.5.4. Ion chromatography (IC)

The samples from the kinetic study were analyzed by the ion-chromatography instrument. Magnesium (Mg<sup>2+</sup>) analyses were conducted in an ion chromatography system (Metrohm 850 Professional IC AnCat-MCS and 858 Professional Sample Processor) with a Metrosep C4-150/4.0 cation exchange column. The eluent contained dipiconilic acid (117 mg·L $^{-1}$ ) and nitric acid (1.7 mmol·L $^{-1}$ ). The system flux was set to 0.9 mL·min $^{-1}$ , and the temperature was 30°C.

#### 2.5.5. Atomic absorption spectroscopy (AAS)

Atomic absorption spectroscopy was used to determine the content of Cd in the post-cementation liquor. The instrument used to perform the analyses was the atomic absorption AA-700 system (Shimadzu), equipped with a Cd hollow cathode lamp (Hamamatsu Photonics K.K.), with the following specifications: a low current peak of 8 mA, a high current peak of 100 mA, and a wavelength of 228.80 nm with an Air-C<sub>2</sub>H<sub>2</sub> flame type, a C<sub>2</sub>H<sub>2</sub> flow rate of 1.8  $L \cdot min^{-1}$  with a burner height of 7 mm and a slit width of 0.7 nm.

#### 3. Results and discussion

#### 3.1. Thermodynamic simulation of leaching parameters

#### 3.1.1. Magnesium extraction

The thermodynamic simulations were performed with the aid of FactSage software version 7.2. According to the databases available in FactSage software, a simulation of the leaching process of dolomite using sulfuric acid and the assessment of the temperature effects on the leaching yield was possible to perform. The databases contain a calculation of energy activation and Gibbs free energy for all possible compounds that may be formed [1,30–33]. They also involve reactions in aqueous media. Figure 2 shows the first set of simulation

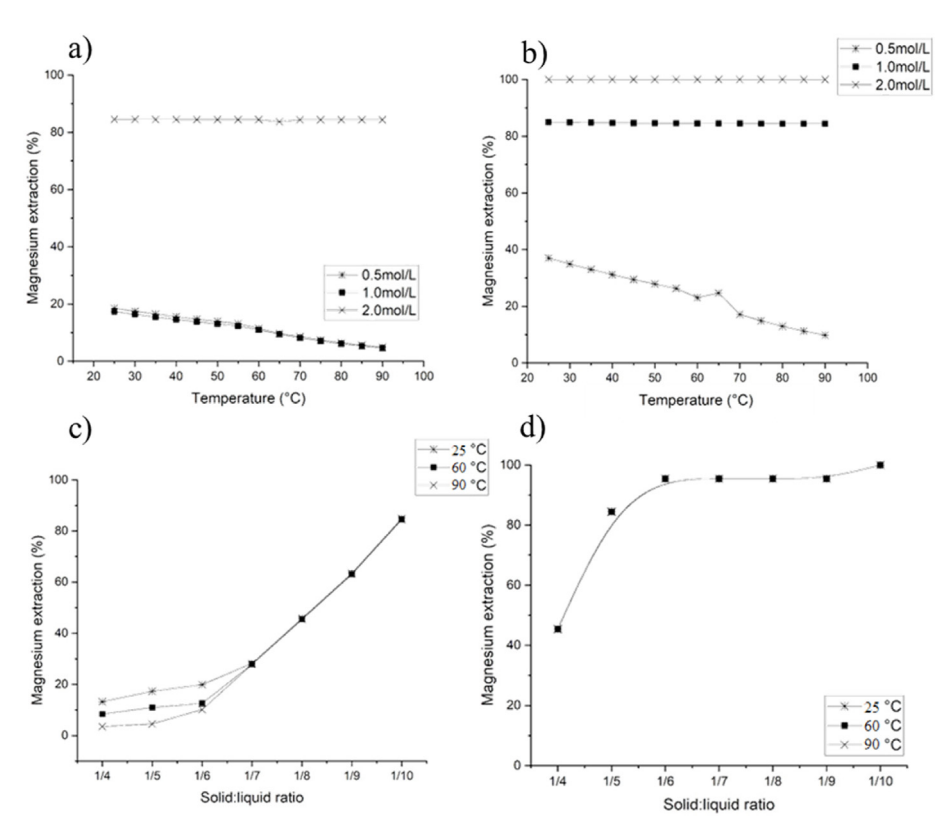


Fig. 2. Modeled magnesium extraction for (a) S:L = 1:5; (b) S:L = 1:10; (c)  $1 \text{ mol·}L^{-1} H_2SO_4$ ; (d)  $2 \text{ mol·}L^{-1} H_2SO_4$ ;

results that evaluated the H<sub>2</sub>SO<sub>4</sub> concentration, solid:liquid ratio, and temperature variation to optimize the conditions of Mg leaching from dolomite. According to Ramalingom et al. (2001) [34], the MgSO<sub>4</sub> has a greater solubility until 90°C. Above this temperature, it becomes insoluble and starts to precipitate as MgSO<sub>4</sub>. Hence, the temperature range chosen for this simulation varied from 25 to 90°C.

The simulation shown in Figure 2a was carried out with an S:L ratio equal to 1:5 that evaluated thermodynamic behavior in H<sub>2</sub>SO<sub>4</sub> concentrations of 0.5-1.0-2 mol·L<sup>-1</sup>. None of the conditions reached 100% extraction. Also, a low Mg extraction was observed, mainly at 0.5 and 1.0 mol·L<sup>-1</sup>, with an extraction of around 20% in temperatures below 50°C. As expected, increasing the temperature to 90°C, the Mg extraction percentage decreased to 1%. Thus, under stoichiometric conditions with an S:L ratio equal to 1:5, magnesium sulfate shows an extraction below 10% even at temperatures below 90°C. From Figure 2a, the temperature effects showed no or little influence on Mg extraction. Besides, the Mg extraction for S:L = 1:5 was lower than 20% for all modeled temperatures when considering  $0.5 \text{ and } 1.0 \text{ mol} \cdot \text{L}^{-1} \text{ H}_2 \text{SO}_4.$ 

Differently from the first simulation, in Figure 2b, an Mg extraction of 100% was achieved using

2.0 mol·L-1  $H_2SO_4$  and an S:L=1:10. At  $25^{\circ}C$  the percentage extraction for 0.5 and 1.0 mol·L<sup>-1</sup> were 85 and 40%, respectively. According to the stoichiometry reaction (1), at least 1 mol·L-1 of H<sub>2</sub>SO<sub>4</sub> is used to react with dolomite in an S:L = 1:10 ratio, then allowing the Mg leaching. It was observed that the highest Mg extraction was in an acid concentration of 2.0 mol·L<sup>-1</sup> (Fig. 2b and c). Further, the MgSO<sub>4</sub> solubility increases in temperatures between 25 and 60°C. Despite that, at temperatures above 60°C, the MgSO<sub>4</sub> is re-precipitated, as shown in Figure 2a and b [34,35]. Also, in Figure 2c the condition of 1.0 mol·L<sup>-1</sup> H<sub>2</sub>SO<sub>4</sub> in the range of S:L ratio from 1:4 to 1:10 was evaluated. Even using the highest ratio, the maximum Mg extraction was around 80%. The temperature has shown no influence on the extraction in S:L ratios from 1:7 to 1:10 as confirmed in Figure 2c and d. The S:L ratio effect is shown in Figure 2d fixing the H<sub>2</sub>SO<sub>4</sub> concentration in 2.0 mol· $L^{-1}$ . The ratios from 1:6 to 1:9 for the extraction were close to 100%. Therefore, only in the simulations results comprising a 1:10 ratio, 100% extraction was reached. In this case, the temperature had no influence on any of the S:L ratios.

Noticed from the previous results that 2  $\text{mol} \cdot \text{L}^{-1} \text{ H}_2\text{SO}_4$  in an S:L ratio equal to 1:10 was accomplishable to obtain a 100% Mg extraction. The

effect of  $H_2SO_4$  concentrations for both S:L ratios equal to 1:5 and 1:10 was investigated, as shown in Figure 3a and b.

The results from Figure 3a demonstrate that for an S:L ratio equal to 1:5, the Mg extraction increased linearly when increasing the acid concentration from 1.2  $\text{mol} \cdot \text{L}^{-1}$  to 2.0  $\text{mol} \cdot \text{L}^{-1}$ , while Figure 3b indicates that for an S:L ratio of 1:10 the Mg extraction achieved a maximum value for 1.2  $\text{mol} \cdot \text{L}^{-1}$  H<sub>2</sub>SO<sub>4</sub> remaining near 100% for all subsequent S:L ratios. Thus, if the S:L ratio is lower than 1:10, the acid concentration must be increased, according to the stoichiometry presented in Equation (1).

By analyzing the results from Figures 2a—d and 3a—b, the optimal parameters for the leaching experimental tests with pure dolomite were established as follows:

- S:L = 1:10 and H<sub>2</sub>SO<sub>4</sub> concentration equal to 1.2 mol·L<sup>-1</sup>, allowing to use less concentrated leaching agent and reach a 100% Mg extraction according to the modeled results shown in Figure 3b. Despite that, experimental leaching tests using higher H<sub>2</sub>SO<sub>4</sub> concentrations were carried out to validate the results.
- Temperature = 25°C, since increasing temperature does not influence the Mg extraction.
   Similarly, experimental leaching essays were performed at higher temperatures to validate the results.

#### 3.1.2. Calcium extraction

Considering that the predominant material of Zn tailing is dolomite (90.3 wt.%), the reaction with H<sub>2</sub>SO<sub>4</sub> would produce MgSO<sub>4</sub>, which has a higher solubility at temperatures between 50 and 80°C and

has  $CaSO_4$  considered insoluble. The phases formed by calcium sulfate are mostly gypsum and anhydrite; for example, at temperatures between 75 and  $100^{\circ}$ C, the anhydrite phase is formed [34,36,37]. The thermodynamic simulation for Ca extraction in different temperatures,  $H_2SO_4$  concentrations, and S:L ratios are shown in Figure 4a—d.

It can be noticed from Figure 4a that the temperatures had no influence on Ca extraction. Besides, due to the low solubility of calcium sulfate, less than 0.25% Ca extraction was obtained. Using an S:L ratio equal to 1:10 the Ca extraction increased to 1% in temperatures from 50 to 90°C as presented in Figure 4b. Even modeling the conditions that could increase the Ca extraction, such as varying the S:L ratio, the yield of Ca extraction was lower than Mg, as presented in Figure 4c and d. The Ca extraction in function of temperature was evaluated from 25 to 90°C in three different acid concentrations. Then, the highest extraction yield was around 1% with 2 mol·L $^{-1}$  H<sub>2</sub>SO<sub>4</sub> at 90°C and an S:L ratio equal to 1:10 (Fig. 4b).

The S:L ratio intervals study in two concentrations of  $H_2SO_4$  (1.0 mol·L<sup>-1</sup> and 2.0 mol·L<sup>-1</sup>) is presented in Figures 4c and d. For 1.0 mol·L<sup>-1</sup>  $H_2SO_4$ , the Ca extraction was close to 0%, even increasing the S:L ratio and temperature. Due to the solubilities of CaSO<sub>4</sub> and MgSO<sub>4</sub> differences, the simulation indicated the possibility to separate calcium sulfate and magnesium sulfate, being advantageous in this dissimilarity, obtaining two by-products from Zn tailing.

FactSage simulation showed the data was compatible with the above-mentioned information about Ca phases. The simulations with temperatures above 75°C suggested the anhydrite formation as expected. The behavior of Ca extraction using an excess of acid was also studied, as indicated in

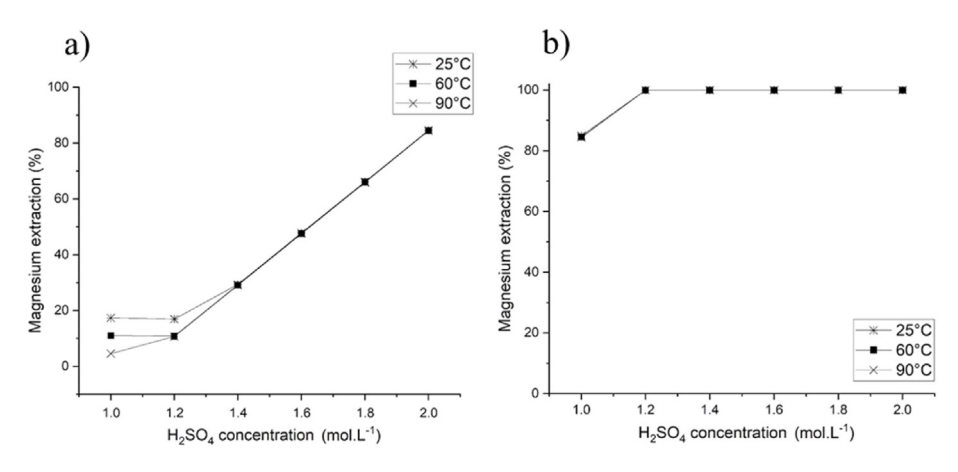


Fig. 3. Modeled magnesium extraction for (a) S:L = 1:5 and (b) S:L = 1:10.

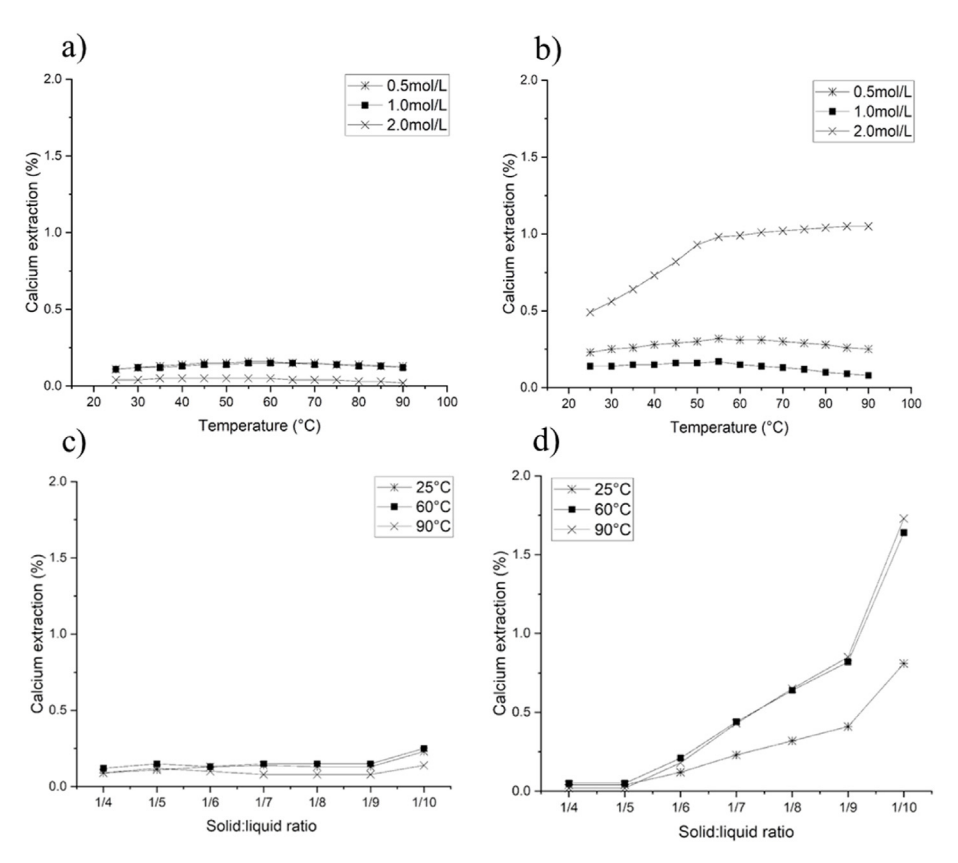


Fig. 4. Modeled calcium extraction for (a) S:L = 1:5; (b) S:L = 1:10; (c)  $1 \text{ mol} \cdot L^{-1} H_2SO_4$ ; (d)  $2 \text{ mol} \cdot L^{-1} H_2SO_4$ ;

Figure 5a and b. Neither temperature nor acid concentration increased the Ca extraction using an S:L ratio = 1:5 (Fig. 5a). On the other hand, when simulating an S:L ratio = 1:10, a subtle variation was observed. Despite the Ca extraction increase with an S:L ratio = 1:10, the modeled results merely reach 1%, as presented in Figure 5b.

To evaluate the leaching of Mg, Ca extraction was also assessed (Fig. 5b), following the set conditions:

1.2 mol·L<sup> $^{-1}$ </sup> H<sub>2</sub>SO<sub>4</sub>, S:L = 1:10, and  $T = 25^{\circ}$ C. Evaluating an excess of acid equivalent to 20% using 1.2 mol·L<sup> $^{-1}$ </sup>, the Ca extraction was below 0.5% for all simulated temperatures.

Thus, as indicated in the simulations from Mg leaching with the following conditions of  $1.2 \text{ mol} \cdot \text{L}^{-1} \text{ H}_2 \text{SO}_4$  at  $25^{\circ}\text{C}$ , and an S:L ratio equal to 1:10 would produce soluble MgSO<sub>4</sub> and insoluble CaSO<sub>4</sub> (gypsum or anhydrite).

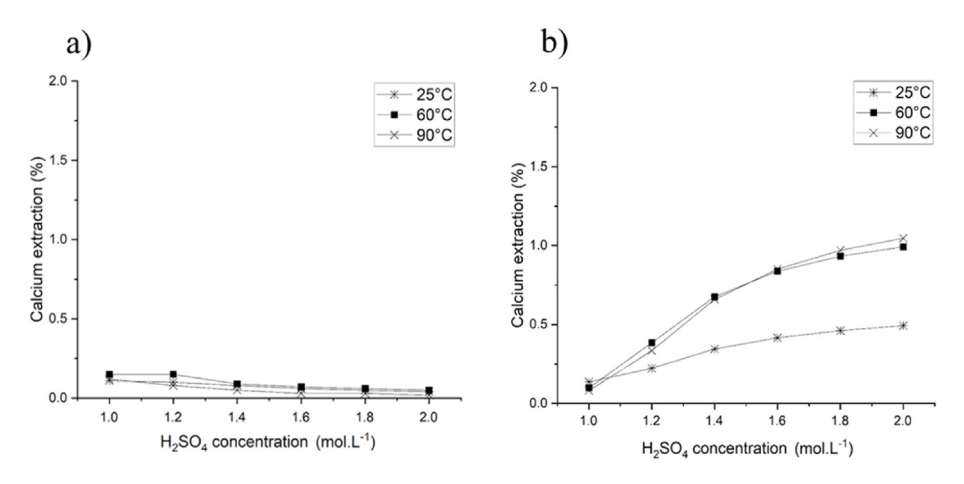


Fig. 5. Modeled calcium extraction for (a) S:L = 1:5 and (b) S:L = 1:10.

## 3.1.3. Thermodynamic simulation for non-magnetic fraction from Zn tailing

The simulations considering the Zn tailing composition (non-magnetic fraction), such as previous results found in Vinhal et al. (2020) [26], aimed to analyze the behavior of the elements found in the material, not only Mg and Ca. Particularly, attention was paid to impurities and toxic metals that can be found in real tailings, focusing on identifying which elements may be soluble or not in the leach liquor (MgSO<sub>4</sub>) or remaining in the non-leached fraction (CaSO<sub>4</sub>). The extraction of Mg, Ca, Pb, Cd, Fe, Zn, and Al were assessed for a range of H<sub>2</sub>SO<sub>4</sub> concentrations and temperature from 25 to 90°C, fixing the S:L ratio in 1:10. These conditions were set based on the previous simulations with pure dolomite.

The results from the simulations with an optimized effect on the Mg extraction are presented in Figure 6a—c. In Figure 6a even with the elements' interference (such as: Ca, Fe, Zn, Al, Pb, and Cd), Mg had the highest leaching yield at 25°C, showing 40% extraction. It was also observed that Cd and Pb had almost zero extraction following the same behavior of the Fe, Al, Ca, and Zn at temperatures higher than 60°C.

Figure 6b shows that increasing the acid concentration to  $1 \text{ mol} \cdot \text{L}^{-1}$ , such as Mg and Cd, had a 100% extraction, particularly above  $60^{\circ}\text{C}$ . Calcium followed the same behavior as the previous simulations with an extraction close to zero, and Pb followed the same trend. Both elements, Ca and Pb, have low solubility as sulfate, differently from Mg and Cd.

According to Apelblat and Korin (2007) [38], Cd as  $CdSO_4 \cdot 8/3H_2O$  phase and at temperatures above  $44^{\circ}C$  becomes cadmium sulfate monohydrate ( $CdSO_4 \cdot H_2O$ ). Based on studies, at higher temperatures ( $1000^{\circ}C$ ), phases that are associated with  $CdSO_4$  decompose, obtaining a  $2CdO \cdot CdSO_4$  phase [39]. Some cadmium phases, such as  $CdSO_4$ ,  $CdSO_4 \cdot 8H_2O$ , and  $CdSO_4 \cdot H_2O$  have a solubility equal to  $767 \text{ g} \cdot \text{L}^{-1}$  ( $T = 25^{\circ}C$ ) [40].

In Figure 6b, the simulation carried out has a divergence with the Mg extraction when compared with the modeled Mg leaching from pure dolomite in Figure 3b. The non-magnetic fraction of the Zn tailing (90.3% dolomite) achieved a 100% Mg extraction using 1.0 mol·L<sup>-1</sup> H<sub>2</sub>SO<sub>4</sub> due to the smaller mass of dolomite. The simulations with pure dolomite achieved 100% Mg extraction using

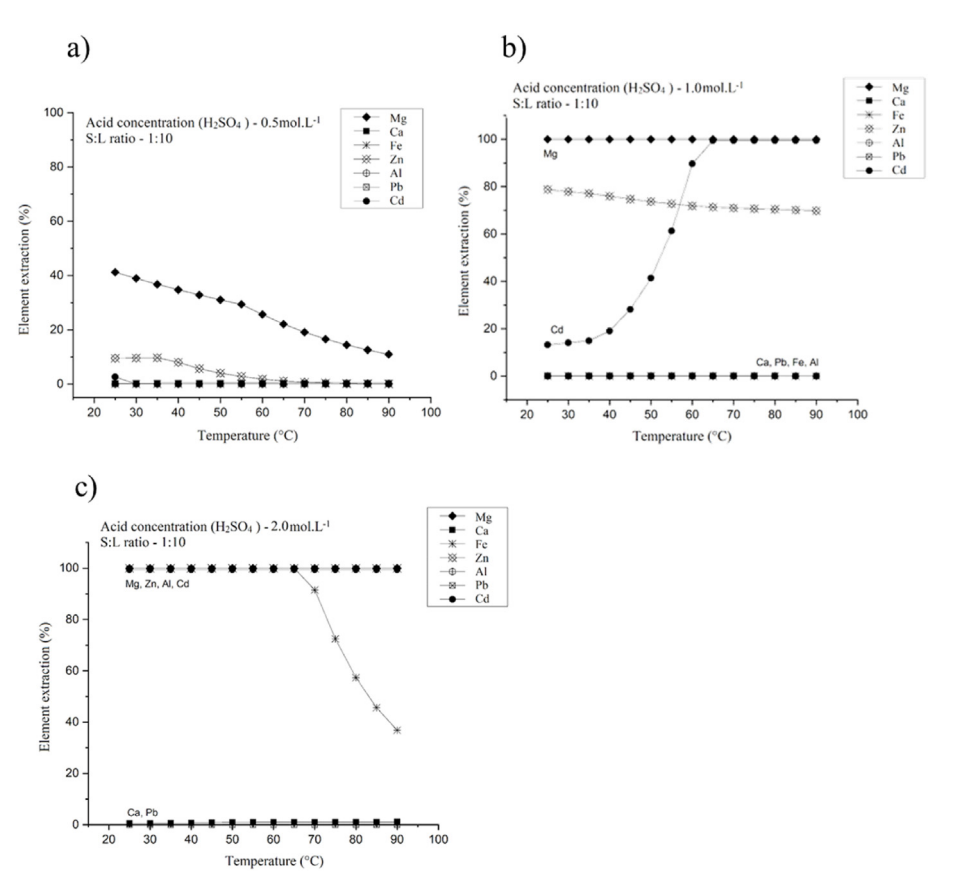


Fig. 6. Modeled Zn tailing for Mg, Ca, Fe, Zn, Al, Pb, and Cd extraction with S:L = 1:10 for (a) 0.5  $mol \cdot L^{-1}$  H<sub>2</sub>SO<sub>4</sub>; (b) 1.0  $mol \cdot L^{-1}$  H<sub>2</sub>SO<sub>4</sub>; (c) 2  $mol \cdot L^{-1}$  H<sub>2</sub>SO<sub>4</sub>.

1.2  $\text{mol} \cdot \text{L}^{-1} \text{ H}_2 \text{SO}_4$ , while the non-magnetic fraction from Zn tailing was possible to reach a 100% extraction using 1.0  $\text{mol} \cdot \text{L}^{-1} \text{ H}_2 \text{SO}_4$ . The behavior of some elements, such as Ca and Pb with 2.0  $\text{mol} \cdot \text{L}^{-1} \text{ H}_2 \text{SO}_4$  was the same, achieving a percent equal to zero of extraction over the range temperature chosen (25–90°C), as presented in Figure 6c. Both Figure 6b and c suggested that the non-leached fraction generates a predominance of CaSO<sub>4</sub> and a Pb phase.

As shown in Figure 6c, the elements, in particular the Zn, Al, and Cd, reached a 100% extraction along with Mg, and Fe presented a 100% extraction until 65°C. From 65 to 90°C, Fe extraction decreased to values lower than 40%. Therefore, Fe<sup>2+</sup> was oxidized to Fe<sup>3+</sup>, which may be explained by the presence of CO<sub>2</sub> in the reaction of dolomite and sulfuric acid. The solubility of Fe<sup>2+</sup> is 7.2 g·L<sup>-1</sup>, and Fe<sup>3+</sup> is considered insoluble [40,41]. This may explain the

possibility for Fe to decrease its extraction, as shown in Figure 6c, also because of the reaction that can change the pH system and allow Fe in the ionic form [42].

FactSage software provided the thermodynamically favored phases supposedly formed in the non-leached fraction along the studied temperature range that were summarized in Tables 1–3.

Table 1 details the amount of Mg that was not leached would form the solid phases:  $CaMg(CO_3)_2$ ,  $MgCO_3$ , and  $Mg_5Al_2Si_3O_{10}(OH)_8$ . Simulations of dolomite did not obtain complete solubilization in temperatures from 25 to 90°C (conditions 0.5 mol·L<sup>-1</sup> H<sub>2</sub>SO<sub>4</sub>), as discussed previously. Hence, magnesium carbonate would be formed from the incomplete dissolution of dolomite. Additionally, calcium is initially presented as dolomite and as calcium sulfate. It is found as gypsum  $(CaSO_4(H_2O)_2)$  in temperatures from 25 to 60°C and

Table 1. List of solid phases thermodynamically predicted by Factsage considering  $H_2SO_4$  0.5 mol· $L^{-1}$ , S:L ratio 1:10 and varying temperature from 25 to  $90^{\circ}$  C.

Temperature (°C)	Compounds						
	Ca	Pb	Fe	Mg	Zn	Al	Cd
25	CaSO <sub>4</sub> (H <sub>2</sub> O) <sub>2</sub>	PbSO <sub>4</sub>	Fe <sub>2</sub> O <sub>3</sub>	CaMg(CO <sub>3</sub> ) <sub>2</sub>	ZnCO <sub>3</sub>	$Al_2O_3(H_2O)$	CdCO <sub>3</sub>
30	and CaMg(CO <sub>3</sub> ) <sub>2</sub>			and MgCO <sub>3</sub>			
35				· ·			
40					$Zn_2SiO_4$		
45							
50							
55							
60							
65	CaSO <sub>4</sub> and					$Mg_5Al_2Si_3O_{10}(OH)_8$	
70	$CaMg(CO_3)_2$						
75							
80							
85							
90							

Table 2. List of solid phases thermodynamically predicted by Factsage considering  $H_2SO_4$  1.0 mol·L<sup>-1</sup>, S:L ratio 1:10 and varying temperature from 25 to  $90^{\circ}$  C.

Temperature (°C)	Compounds							
	Ca	Pb	Fe	Zn	Al	Cd		
25	CaSO <sub>4</sub> (H <sub>2</sub> O) <sub>2</sub>	PbSO <sub>4</sub>	Fe <sub>2</sub> O <sub>3</sub>	ZnCO <sub>3</sub>	Al <sub>2</sub> O <sub>3</sub> (H <sub>2</sub> O)	CdCO3		
30								
35								
40				$Zn_2SiO_4$	$Al_2O_3(H_2O)$			
45								
50								
55	$CaSO_4$							
60								
65								
70								
75								
80								
85								
90								

Table 3. List of solid phases thermodynamically predicted by FactSage considering  $H_2SO_4$  2.0  $mol\cdot L^{-1}$ , S:L ratio 1:10 and varying temperature from 25 to 90°C.

Temperature (°C)	Compounds				
	Ca	Pb	Fe		
25	CaSO <sub>4</sub> (H <sub>2</sub> O) <sub>2</sub>	PbSO <sub>4</sub>	Fe <sub>2</sub> O <sub>3</sub>		
30					
35					
40					
45					
50					
55	$CaSO_4$				
60					
65					
70					
75					
80					
85					
90					

as anhydrite (CaSO<sub>4</sub>) in temperatures from 65 to 90°C, which means that while the temperature increases, the composition loses water.

The simulation using the following conditions of  $0.5 \text{ mol} \cdot \text{L}^{-1} \text{ H}_2 \text{SO}_4$  shows that more compounds are formed in the non-leached fraction, compared with simulations conditions of  $1.0 \text{ and } 2.0 \text{ mol} \cdot \text{L}^{-1} \text{ H}_2 \text{SO}_4$  as shown in Table 1. In this case, Cd was formed as a carbonate after the addition of sulfuric acid, while Pb was formed as a sulfate — independently of the temperature set. Another element found as a carbonate was Zn at a  $T = 25-35^{\circ}\text{C}$  and as a silicate at

 $T = 40-90^{\circ}$ C. The Fe remained as hematite in all temperatures.

It is observed that increasing the  $\rm H_2SO_4$  concentration to 1.0  $\rm mol\cdot L^{-1}$  has resulted in phases listed in Table 2. It was observed that dolomite is no longer present in the non-leached fraction. Other compounds are formed in conditions presented in Table 2, except for Mg, which achieved 100% extraction.

In Table 3, the condition used was  $2 \text{ mol} \cdot \text{L}^{-1} \text{ H}_2 \text{SO}_4$ , and then phases with Ca, Pb, and Fe was presented in the non-leached fraction. Due to the difference in the temperature, calcium sulfate was acquired in two phases: gypsum (CaSO<sub>4</sub>(H<sub>2</sub>O)<sub>2</sub>) and anhydrite (CaSO<sub>4</sub>). The Fe remained as hematite and Pb as sulfate. In this case, even when increasing the concentration of sulfuric acid, these compounds' behavior is set as insoluble.

### 3.1.4. Eh-pH diagrams for thermodynamic modelling of impurities

The thermodynamics of the leaching route considers the chemical equilibrium with all the possible species in every reaction [1]. Through the Eh-pH diagrams and the phases/species formed, it was possible to understand the fate of the impurities from the tailing before the experimental leaching tests. In particular, the behavior of  $PbSO_4$  and  $CdSO_4$  — considered toxic elements — were investigated since their presence must be avoided in leach liquor. Figure 7 shows the Eh-pH diagram

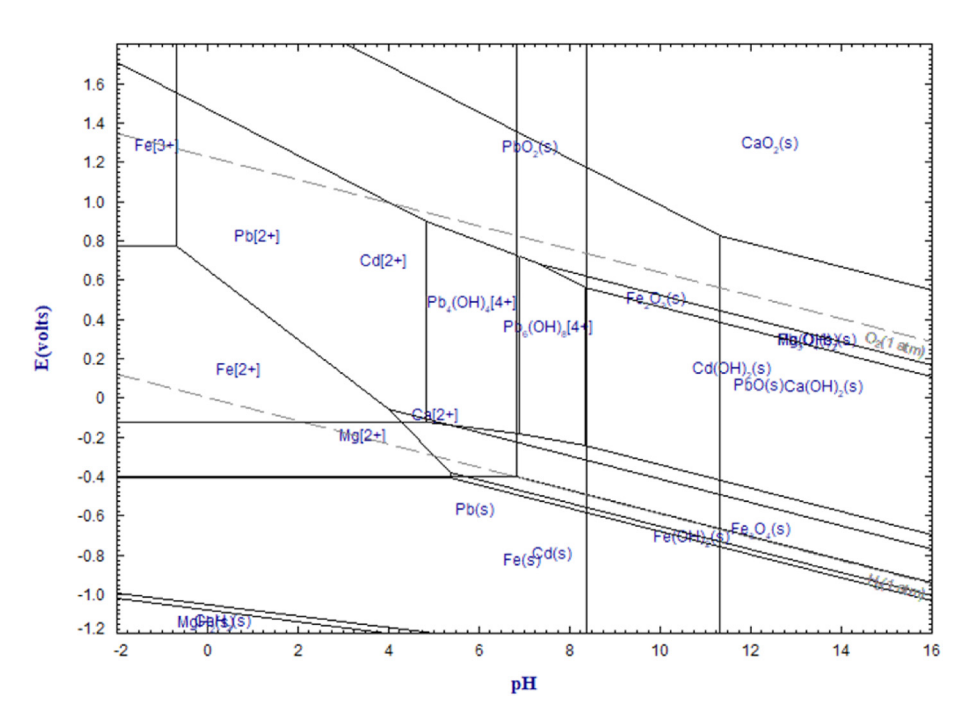


Fig. 7. Speciation diagram - FactSage EpH module with the main compounds of the non-magnetic Zn flotation tailing.

assembled according to the composition of the nonmagnetic fraction from Zn tailing.

In addition to Figure 7, it is observed that Cd assumes its ionic form in an aqueous medium [Cd<sup>2+</sup>] in the same pH range as  $Mg^{2+}$  and  $Pb^{2+}$  (pH 0 to 4) at 25°C. This contrasts with the solubility of CdSO<sub>4</sub> at 25°C, which is around 767 g·L<sup>-1</sup>, while the solubility of PbSO<sub>4</sub> is lower (equal to 0.04 g·L<sup>-1</sup>). Likewise, the solubilities of  $MgSO_4$  and  $CdSO_4$  are approximately 357 g·L<sup>-1</sup> and 2.05 g·L<sup>-1</sup>, respectively [40,43]. Considering the difference in solubilities, the leach liquor is expected to present negligible amounts of Pb. Otherwise, the dissolution of Cd must be considered [34,44,45].

The reactions among the compounds found in the non-magnetic Zn tailing added with sulfuric acid are represented by Equations (2)—(8) as follows:

$$\begin{array}{l} MgCO_{3(s)} + H_2SO_{4(aq)} \leftrightarrow \\ H_2O_{(l)} + CO_{2(g)} + MgSO_{4(aq)} \end{array} \tag{2} \label{eq:2}$$

$$CaCO_{3(s)} + H_2SO_{4(aq)} \leftrightarrow H_2O_{(l)} + CO_{2(g)} + CaSO_{4(s)}$$
 (3)

$$Fe_2O_{3(s)} + 3H_2SO_{4(aq)} \leftrightarrow 3H_2O_{(l)} + Fe_2(SO_4)_{3(s)}$$
 (4)

$$ZnO_{(s)} + H_2SO_{4(aq)} \leftrightarrow H_2O + ZnSO_{4(aq)}$$
 (5)

$$Al_2O_{3(s)} + 3H_2SO_{4(aq)} \leftrightarrow 3H_2O_{(l)} + Al_2(SO_4)_{3(aq)}$$
 (6)

$$CdO_{(s)} + H_2SO_{4(aq)} \leftrightarrow H_2O_{(l)} + CdSO_{4(aq)}$$
 (7)

$$PbO_{(s)} + H_2SO_{4(aq)} \leftrightarrow H_2O_{(l)} + PbSO_{4(s)}$$
 (8)

#### 3.2. Acidic leaching

The performance of the leaching tests was done to ascertain the results from the thermodynamic simulation and to evaluate the kinetic effects. Besides, the aim was to compare the simulation and the results from leaching tests and then follow the leach liquor to a purification stage.

The leaching agent used was 1.2 mol·L<sup>-1</sup> H<sub>2</sub>SO<sub>4</sub> solution — as indicated by simulations (item 3.1). The S:L ratio was fixed at 1:10 for all assays. Figures 8a and b shows the acidic leaching of Mg and other elements from the non-magnetic fraction using H<sub>2</sub>SO<sub>4</sub>. Figures 8a shows the Mg extraction percentage as a function of time and temperature. According to Figure 8a, after 60 min, the Mg extraction was directed to stabilize. The extraction was lower at 25°C when compared to other temperatures until 50 min. Then, it stabilized at similar yields.

Also, based on Figure 8a, the Mg extraction using 1.2 mol·L<sup>-1</sup> H<sub>2</sub>SO<sub>4</sub> achieved higher rates after approximately 30–50 min. After 60 min, a slight decrease was noticed. This trend follows the simulated results, which have shown that increasing the temperature could result in lower extraction rates due to the Mg precipitation. Aside from the temperature, the reaction time appears to influence Mg precipitation. The tests performed at 25°C showed a lower extraction percentage than others up to 50 min when an extraction rate was close to other evaluated temperatures. The parameters with the highest yield result of Mg extraction were at 35 min and 50°C, leading to an Mg extraction of 72% ±5%.

Figure 8b shows the effect of acid concentration aiming to provide an excess of acid, which was also studied. From the stoichiometric reaction presented in Equation (1), five different acid concentrations

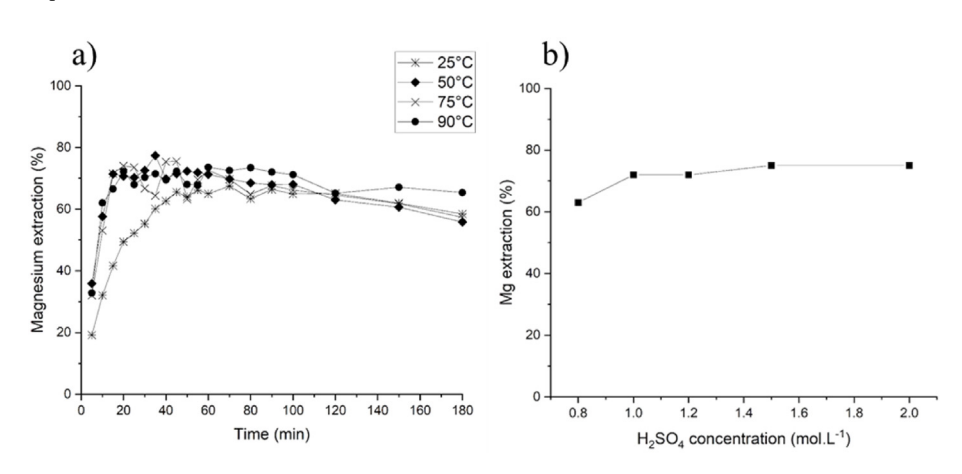


Fig. 8. Acidic leaching of the non-magnetic fraction using  $H_2SO_4$ : (a) yield of Mg extraction in relation to temperature and time; (b) yield of Mg extraction at  $50^{\circ}$ C in 35 min.

were evaluated and compared (0.8, 1.0, 1.2, 1.5, and  $2.0 \text{ mol} \cdot \text{L}^{-1}$ ). The condition using 1.0  $\text{mol} \cdot \text{L}^{-1}$  represents the stoichiometric relation between  $\text{H}_2\text{SO}_4$  and dolomite/tailing. The conditions using 1.2–1.5–2.0  $\text{mol} \cdot \text{L}^{-1}$  provided an acid excess of 20, 50, and 100%, respectively. From 1.0 to 2.0  $\text{mol} \cdot \text{L}^{-1}$ , the Mg extraction showed a yield above 60%. The highest Mg extraction was reached using 1.5 and 2.0  $\text{mol} \cdot \text{L}^{-1}$  H<sub>2</sub>SO<sub>4</sub>, being around 75–80%.

From the results shown in Figure 8b, no significant variation in Mg extraction was observed. Therefore, an excess of acid equal to 20% was chosen to proceed with the experimental tests.

Thus, the optimal conditions for Mg extraction from dolomite in the non-magnetic fraction of the tailing were  $1.2 \text{ mol} \cdot \text{L}^{-1} \text{ H}_2 \text{SO}_4$ , 35 min, and  $50^{\circ}\text{C}$ .

The results from the acidic leaching were compared to simulations achieved by FactSage. It was observed that the Mg leaching had a lower extraction yield than was expected from the simulation. In simulations, the kinetic effects are not considered but may have influenced the results by decreasing the Mg extraction in the experimental test. Another hypothesis that may explain the differences in Mg extraction yield is the lower availability of SO<sup>4-</sup> in the leaching solution after gypsum (CaSO<sub>4</sub>) was formed. Hence, a lower rate of Mg extraction and a slight difference in the optimal leaching temperature was observed during the experiment (leaching test). Nevertheless, the simulations proved to be a reliable basis for selecting the experimental parameters for the leaching test.

Additionally, Ca was virtually not detected in the leach liquor following the thermodynamic simulation and the reaction described in Equation (1).

Subsequently, a new set of leaching tests with  $H_2SO_4$  concentrations from 0.8 to 1.5 mol·L<sup>-1</sup> were performed at  $50^{\circ}$ C in 35 min, also evaluating the fate of other elements. The analysis results from both leach liquor and non-leached fraction are shown in Figure 9a and b.

The results presented in Figure 9a are from a quantitative analysis of the leach liquor. It is observed that Ca, Pb and Al have a low extraction (< 5%), as expected. On the other hand, Mg and Cd had an extraction above 60% in all the conditions of  $H_2SO_4$  — from 1.0 mol·L<sup>-1</sup>. Some other similarity from the simulation was the Fe and Zn extraction being around 10% and  $\geq 50\%$ , respectively.

The pH was monitored during the assays, as presented in Table 4. The compounds obtained as solid/precipitated were  $CaSO_4$  and  $PbSO_4$  in the non-leached fraction, while Cd was solubilized along with Mg at pH < 2. Some challenges during the leaching of dolomite were found due to the control of partial pressure  $CO_2$  generated – reaction with  $CaMg(CO_3)_2$  and  $H_2SO_4$ , as well as the pH measurement. There is a disparity in the values of the solubility product of dolomite in an acid medium above room temperature [36,46].

Although under the proposed conditions, the leaching step showed to be efficient in the extraction of Mg from dolomite with the presence of impurities detected in the leach liquor, especially Cd. The

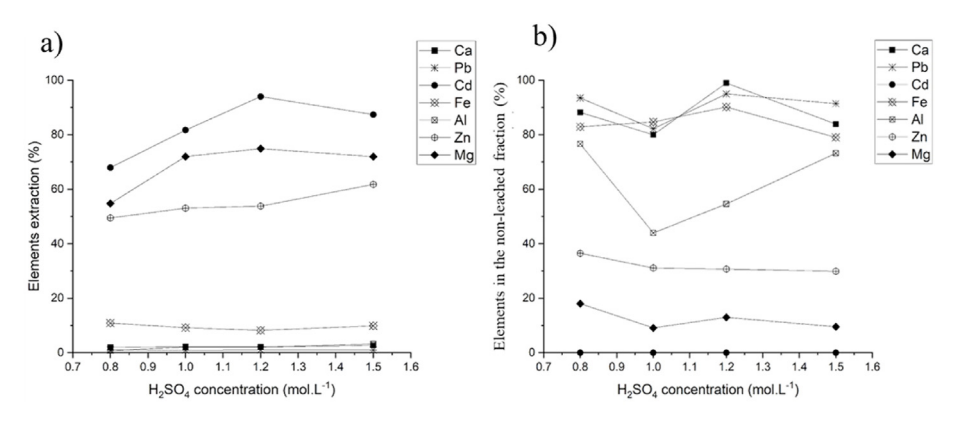


Fig. 9. Acidic leaching of the non-magnetic fraction using  $H_2SO_4$ : (a) yield of elements extraction at  $50^{\circ}$ C in 35 min in leach liquor; (b) elements in the non-leached fraction at  $50^{\circ}$ C in 35 min.

Table 4. Molar concentration of H<sub>2</sub>SO<sub>4</sub> acid in leaching and pH in 5, 20, and 35 min.

	$0.8~{ m mol}\cdot{ m L}^{-1}$	$1.0~{ m mol}\cdot { m L}^{-1}$	$1.2 \text{ mol} \cdot \text{L}^{-1}$	$1.5~\mathrm{mol}\cdot\mathrm{L}^{-1}$	$2.0 \text{ mol} \cdot \text{L}^{-1}$
pH <sub>5min</sub>	0.94	0.68	0.59	0.66	1.05
pH <sub>20min</sub>	1.66	0.91	0.57	0.62	0.67
pH <sub>35min</sub>	2.46	1.13	0.63	0.60	0.57

chemical analyses have shown that the leach liquor with 1.2  $\text{mol} \cdot \text{L}^{-1}$   $\text{H}_2\text{SO}_4$  presented 400  $\text{mg} \cdot \text{L}^{-1}$  of Cd. The non-leached fraction analyses showed that 100% of Cd was solubilized.

For a better investigation of the formed phases, XRD and SEM-EDS analyses were performed with the non-leached fraction (Figs. 10 and 11). Figure 10 shows the peaks 1 and 2 indicating the formation of calcium sulfate phases,  $Ca(SO_4) \cdot 2H_2O$ , in all evaluated  $H_2SO_4$  concentrations.

The same characteristic peak of calcium sulfate phases is observed in a study by Tolonen et al. (2015) [47].

According to the SEM-EDS in Figure 11, it is observed that the surrounding material is distinguished by lamellas, which is a characteristic of

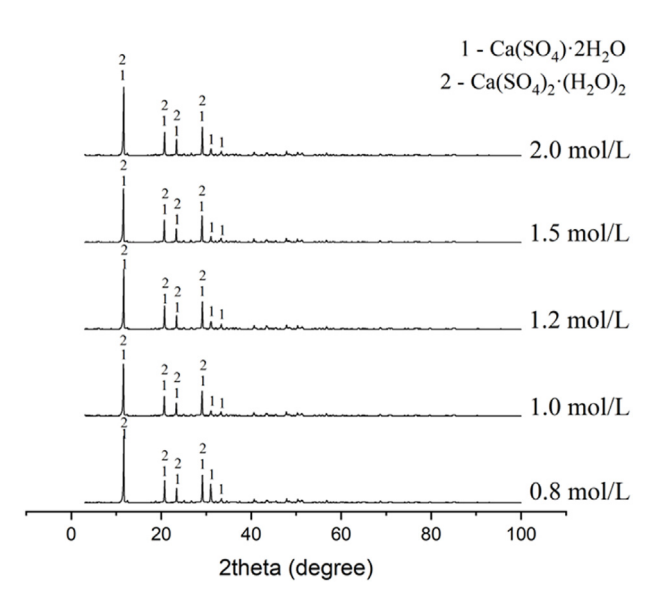


Fig. 10. XRD of the non-leached fraction for acid concentration from 0.8 to  $2.0 \text{ mol-L}^{-1}$ ,  $50^{\circ}\text{C}$  in 35 min.

gypsum or CaSO<sub>4</sub> phases. The particle exhibited a lamellar and spike aspect, with a diameter of around 52.5  $\mu$ m, in a microregion predominantly composed of Ca, S, and O. The SEM-EDS contributed to confirming the presence mainly of Ca in the non-leached fraction.

#### 3.3. Cementation post-treatment

#### 3.3.1. Cementation using synthetic solution

Since the aim of the study is to find alternatives for Zn flotation tailing, the production of MgSO<sub>4</sub> as an alternative was investigated. This by-product could be a potential candidate to be used as fertilizer in agriculture, but it must be considered to remove the remaining Cd of the leach liquor. Thus, cementation was evaluated as a possible post-treatment step (purification).

The cementation of Cd using Zn powder is a well-established method, and it has been evaluated under different conditions [1,48–50]. Then, it was used to investigate its application in mining tailings. Due to the redox process, Zn is less noble than Cd. This is why Zn is oxidized while Cd is reduced. The global reaction is shown in Equation (9).

$$Cd^{2+} + Zn_{(s)} \rightarrow Cd_{(s)} + Zn^{2+}$$
 (9)

The performance of the assays using a synthetic solution containing both Mg and Cd in a sulfuric medium with the same concentration as the leach liquor is presented in Figure 12a and b.

Figure 12a shows the results of the Cd removal during the cementation for different Zn:Cd ratios: 1:1, 2.5:1, 5:1, 10:1, and 100:1 after 20 min. The 100:1 ratio yielded the highest Cd removal, which is equivalent to approximately 100%.

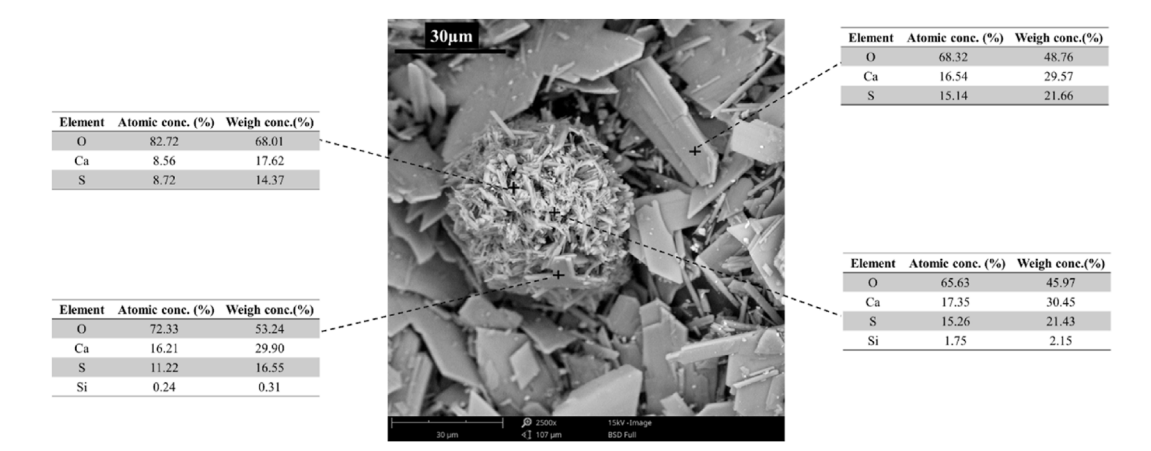


Fig. 11. Backscattered electron (BSE) spot image obtained in the scanning electron microscope and weight composition of the sample, obtained by EDS of the non-leached fraction in 1.2  $mol \cdot L^{-1} H_2SO_4$  in 35 min at 50°C.

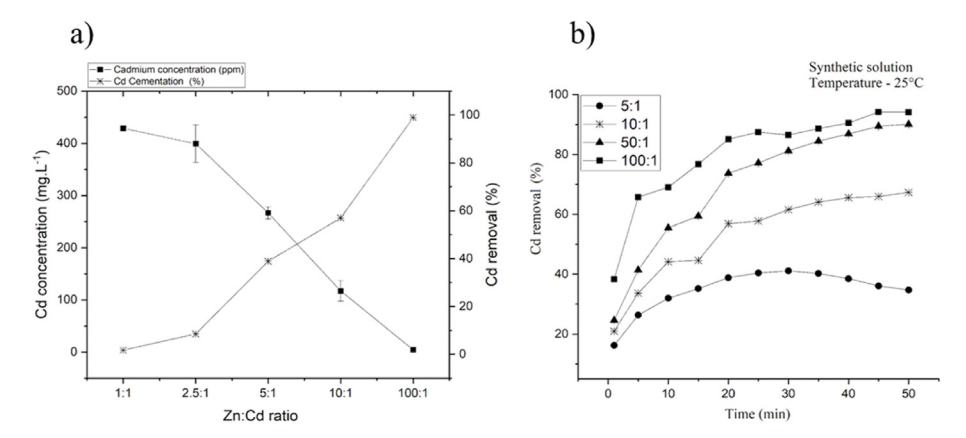


Fig. 12. Cd removal during cementation with synthetic solution containing 400 mg·L $^{-1}$  Cd and 9600 mg·L $^{-1}$  Mg (a) Zn:Cd ratio variation in 20 min (b) 1-50 min for different Zn:Cd ratios.

Also, the second set of tests was performed, and aliquots were withdrawn every 5 min to evaluate the influence of time on Cd cementation. The aliquots were forwarded to chemical analysis. The results are detailed in Figure 12b.

Younesi et al., (2006) [50] found a tendency to increase the removal of Cd in the function of time and a higher Zn:Cd ratio. Similarly, the obtained results are shown in Figure 12a and b. In Figure 12b, it was observed that in all situations, the Cd removal stabilized in 35 min. Particularly in the 50:1 and 100:1 ratio, it was shown that from 35 min, the Cd removal stabilized around 90% (Fig. 12b).

According to Younesi et al., (2006) [50], the increase of Cd cementation in the function of time may be attributed to different mechanisms that control the reaction. The authors reported that different kinetic models might describe the cementation process, depending on the Cd concentration. Such examples were the ash diffusion model, which was suitable for Cd concentrations higher than 100 mg·L<sup>-1</sup> and film diffusion control. Concentrations between 500 mg·L<sup>-1</sup> and 1000 mg·L<sup>-1</sup> provided a mixed kinetic mechanism, while for concentrations below 500 mg·L<sup>-1</sup>, the data adjustment was best for the film diffusion control.

SEM-EDS analysis of Zn powder shows a spherical shape with a diameter of approximately 20  $\mu$ m, in Figure 13a. Also, Figure 13a—f has shown the differences in the Zn powder structure when increasing Zn:Cd ratio. It is observed that the arrangement of spicules as Cd is cemented. These spicules begin to emerge in the lower Zn:Cd ratio Figure 13b and become more evident as the ratio increases. In Figure 13c, a spot region image analysis was performed for a Zn:Cd ratio equal to 5:1, and the presence of Cd was also observed in a concentration lower than the previous ratio (2.5:1) —

due to the EDS identifying a cluster formed by Cd on Zn. Figure 13e refers to the 50:1 Zn:Cd ratio that obtained a Cd removal of 75% in 20 min. Due to the increase of Zn powder mass, the tendency was to increase the removal of Cd. SEM-EDS identified a spot region image of Cd and Mg; the Zn:Cd ratio with the best condition cementation is shown in Figure 13f, which was the sample that contained the largest mass of Zn powder. The EDS analyzed Zn and Cd with a mass concentration equal to 75 and 17%, respectively. Despite that, Cd was cemented, as shown in the spot region imaged by SEM.

#### 3.3.2. Cementation using leach liquor

The leach liquor obtained in the experimental leaching step with the conditions 1.2 mol $\cdot$ L $^{-1}$  H $_2$ SO $_4$  at 50 $^{\circ}$ C in 35 min was used as part of the cementation step, and the effect of the Zn:Cd ratio and time were evaluated. The cementation test results are shown in Figure 14a. Cd removal was studied in different Zn:Cd ratios as a function of time using room temperature (25°C). In Figure 14a the Cd removal was efficient in shorter times when compared with the synthetic solution. Mainly, for Zn:Cd ratio of 100:1 was the closest to removing 100% Cd. The Zn:Cd ratio obtained a removal of around 40%. These two options were shown as insufficient to remove Cd in the leach liquor. Also, it was observed that in 5 min, the Zn:Cd ratios that were equal to 50:1 and 100:1 presented a removal of 70% and above 90%, respectively. While increasing time, the Cd removal decreased for both ratios. The behavior differences between the synthetic solution and the leach liquor may be due to the presence of Fe ( $E^0 = -0.44 \text{ V}_{SHE}$ ) or even the presence of some other elements that may undergo an electrochemical reduction on Zn particles along with Cd [1].

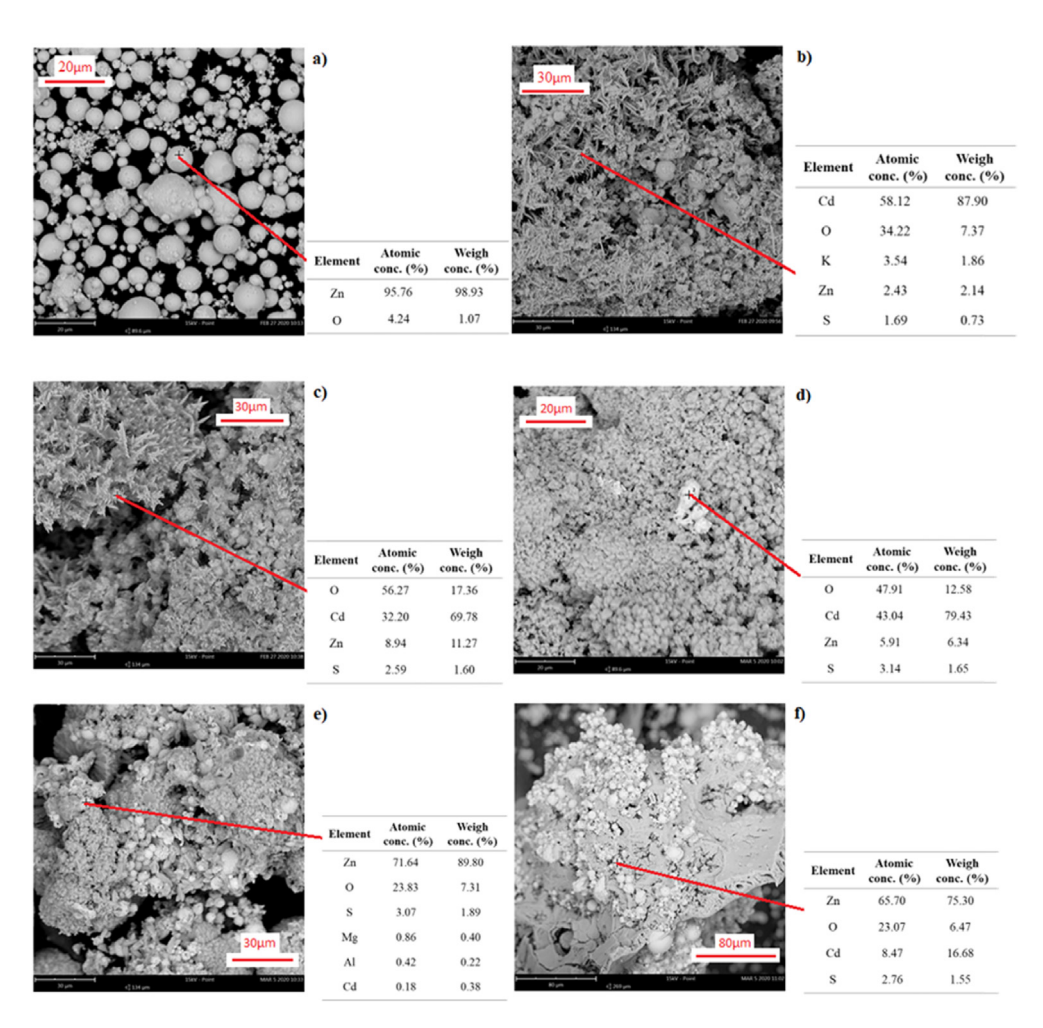


Fig. 13. Backscattered electron (BSE) spot images obtained in the scanning electron microscope and composition of the samples (wt%) obtained by EDS: (a) pure Zn powder before cementation; cementation in 20 min at 25°C with Zn:Cd ratios of (b) 2.5:1; (c) 5:1; (d) 10:1; (e) 50:1; (f) 100:1.

Also, it was analyzed the Mg loss during the cementation step. The results of Mg removal during the cementation are shown in Figure 14b. The Mg removal in cementation is close to zero due to its standard reduction potential ( $E^0 = -2.37$ 

 $V_{\text{SHE}}$ ), which is more negative than Zn ( $E^0=-0.76$   $V_{\text{SHE}}$ ) Thus, it tends to remain in the oxidized state.

For Cd concentrations lower than or equal to  $400~\text{mg}\cdot\text{L}^{-1}$ , the estimative of the amount of Zn is

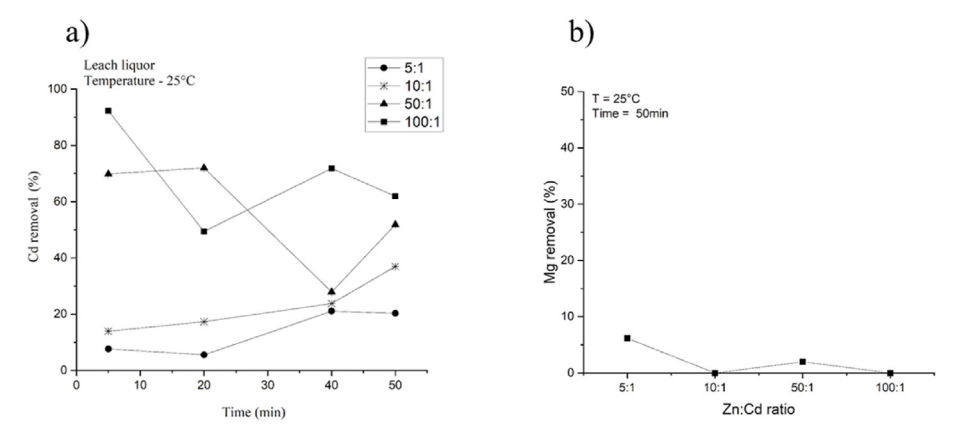


Fig. 14. Results from cementation at room temperature with leach liquor (a) Cd removal as a function of time (b) Mg removal during cementation, after 50 min, for different Zn:Cd ratios.

required for Cd removal and can be calculated as described in Table 5.

Based on the results from Table 5, a theoretical estimative of the concentration of Cd remaining in a solid phase produced by a crystallization method was carried out. Firstly, it was assumed that MgSO<sub>4</sub> crystallization would produce MgSO<sub>4</sub>·7H<sub>2</sub>O at an average yield of 80%, according to previous results from Wanderley et al. (2020) [51]. It was also assumed that all the remaining Cd (i.e., the noncemented Cd) would be structurally incorporated into the solid phase formed. Hence, the lowest calculated amount of Cd was 50 mg·kg<sup>-1</sup> for Condition I, as shown in Table 5.

Standards value of toxic metals in soils, as presented in the Soil Environmental Quality

Table 5. Best cementation conditions (Zn:Cd ratio and time) for the leach liquor with Zn powder in grams per liter of leachate, removal of Cd (%) and remaining Cd in  $mg \cdot kg^{-1}$ .

Condition	Zn:Cd			Remaining Cd (mg/kg)	Cd removal (%)
I	100:1	5	23	50	92
II	50:1	20	11.6	200	72
III	10:1	50	2.32	400	37

Standards (SEQSs), were set out as a criterion for evaluating the possibility of using the Mg-rich liquor obtained after leaching and cementation steps as raw material for agricultural purposes. Countries such as France and Germany have Cd limits equal to 20 mg. kg<sup>-1</sup> in contrast to the USA and Japan, where limits are 37 and 150 mg·kg<sup>-1</sup>, respectively [52].

In Brazil, the maximum limits for toxic metals in agriculture products are established by the Secretary of Agriculture Defense and published by the National Environment Council (CONAMA) according to Resolution 420/2009 [53]. The proposed limit for Cd in secondary macronutrient fertilizers, such as  $MgSO_4$ , is  $20~mg\cdot kg^{-1}$  [53].

By considering the different limits for Cd proposed by each legislation, the produced MgSO<sub>4</sub> could be used mixed with raw fertilizer to reach the toxicity limits. In the case of leach liquor, a study that evaluates the crystallized product should be explored, or a cementation/purification step that is equal to or higher than 96% for Cd removal. The removal of Cd, even with an average of 92%, did not present enough efficiency to be used solely as a fertilizer material.

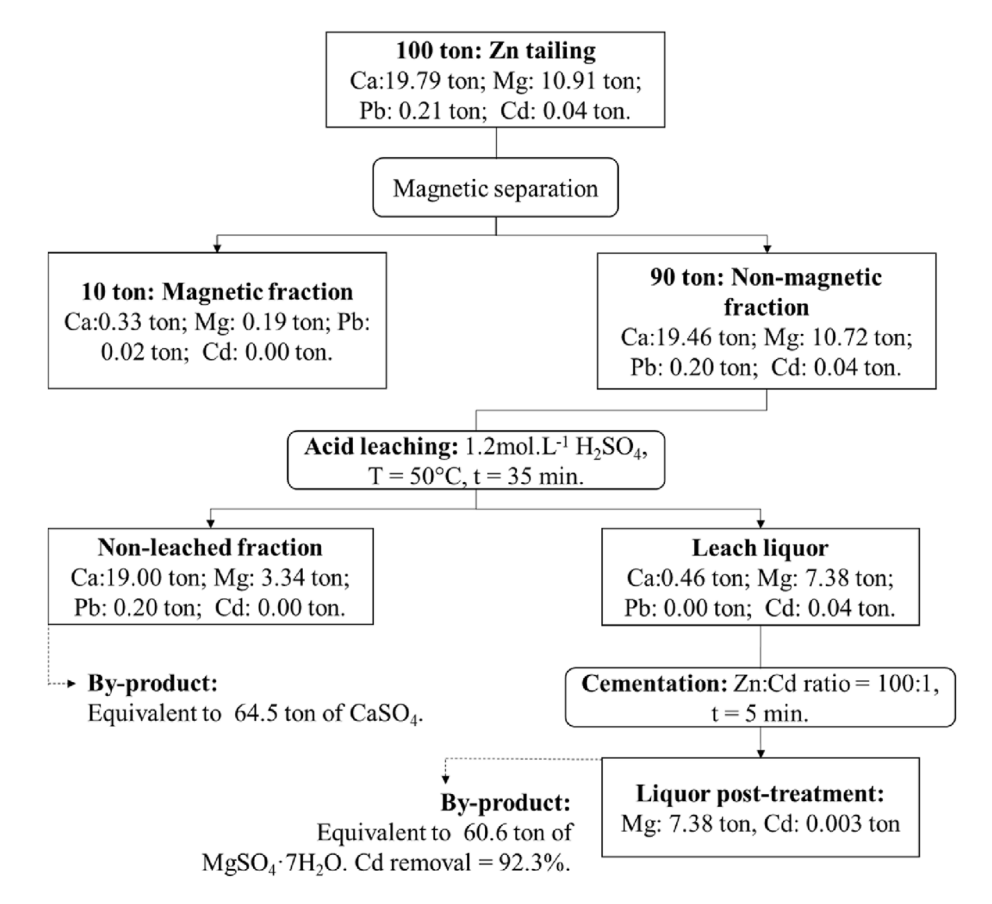


Fig. 15. Material balance of the production of MgSO<sub>4</sub> and CaSO<sub>4</sub> from a Zn flotation tailing considering the proposed route.

However, considering a 92% removal of Cd in the cementation step, it is important to highlight possible studies that may include a new separation/purification step of Cd cemented. Precisely because Cd presents a commercial interest as a manufacturer of materials such as batteries, pigments, coatings, stabilizers for plastics, non-ferrous alloys, and photovoltaic devices, it is widely used in various industrial applications [54]. According to Li et al. (2018) [55], a leach liquor purification method was studied, known as cyclone electrowinning from polymetallic solutions to recovery metals residues considered noble impurities, e.g., Cu<sup>2+</sup>, Cd<sup>2+</sup> and Co<sup>2+</sup>, which can be an alternative to be investigated focusing on obtaining Cd.

#### 3.4. General mass balance

In Figure 15, a flowsheet understanding the mass balance to produce  $MgSO_4$  and  $CaSO_4$  from Zn tailing is presented. In this mass balance, it was considered an input of an initial 100 tons. The first step considered the Zn tailing characterization and physical processing conditions (rougher cleaner) presented in previous work of ours [26]. The second step included the hydrometallurgical route (leaching and cementation), then it was calculated the weight of each obtained by-product —  $CaSO_4$  and  $MgSO_4 \cdot 7H_2O$  [51].

It is worth mentioning that the obtained CaSO<sub>4</sub> remains with Pb equal to 0.20 wt.% or 2000  $mg \cdot kg^{-1}$ . Nevertheless, Brazilian legislation allows the use of gypsum mixed with raw soil conditioner as another alternative up to the maximum established limit for Pb equal to 150  $mg \cdot kg^{-1}$ .

Alternatives to explore and evaluate how to decrease or remove toxic elements from both by-products are encouraged. For the non-leached material by-product, a lead removal study is required — whether by another leaching (hydrometallurgical route) [56], physical processing [57,58], ionic liquids [59], or pyrometallurgy [60,61].

In addition, a calculation can be performed focusing on obtaining more detailed information within the scope of economic accounting based on this process, considering the amount of tailing generated, dolomite concentration and the production of two by-products (Ca and Mg sulfates). In this study, the Zn mine beneficiation is estimated to be 14000 kt/year with a production of Zn tailing equivalent to 100 kt/month, a total of 1200 kt/year, corresponding to 8.6% of tailing in the flotation step generated in the process [62,63]. Moreover, it was obtained using a hydrometallurgical route, a production equivalent to 60.6 tons of MgSO<sub>4</sub>·7H<sub>2</sub>O and

64.5 tons of CaSO<sub>4</sub>. Also, 0.037 tons of Cd was removed and can be purified.

#### 4. Conclusions

The experimental leaching test was able to achieve up to 72%  $\pm 5$ % Mg extraction and 2% Ca extraction using the following parameters:  $1.2 \text{ mol} \cdot \text{L}^{-1} \text{ H}_2 \text{SO}_4$  and S:L = 1:10, at 50°C in 35 min. Thermodynamic simulations were shown to be a reliable basis for planning exploratory essays.

The MgSO<sub>4</sub> and CaSO<sub>4</sub> differences in solubilities allowed the obtention of a soluble Mg-rich  $(9.6 \text{ mg} \cdot \text{L}^{-1})$  leach liquor and a non-leached fraction with insoluble calcium sulfate dehydrate – gypsum.

The cementation step with Zn powder was able to achieve a Cd removal of 92% in the real leach liquor using a Zn:Cd ratio equal to 100:1 in 5 min at 25°C.

Lastly, a mass balance was proposed. The theoretical calculation to obtain the by-products was equivalent to 61 tons of  $MgSO_4 \cdot 7H_2O$  and 64.5 tons of  $CaSO_4$ . Both obtained by-products are potential candidates as a secondary macronutrient for fertilizers ( $MgSO_4 \cdot 7H_2O$ ) and as gypsum for soil conditioners ( $CaSO_4$ ).

The results of the simulation and leaching test are promising in this article, and the main conclusion is that two by-products were obtained from mining tailing. For the non-leached fraction by-product, a lead removal study is required: whether by another hydrometallurgical route, physical processing, ionic liquids, or pyrometallurgy.

#### Ethical statement

The authors state that the research was conducted according to ethical standards.

#### **Funding body**

No external funding was sourced for this work.

#### Conflicts of interest

The authors declare no conflict of interest.

#### Acknowledgments

The authors acknowledge the FAPESP/Capes grants 2012/51871-9, Sao Paulo Research Foundation (FAPESP), for the financial support and acknowledge the Polytechnic School of the University of Sao Paulo — Brazil, SP. This work was also supported by a CAPES/BRAZIL EMBRAPIIscholarship. The information presented in this study is from the authors and does not necessarily reflect the opinions of CNPq, FAPESP, CAPES, or EMBRAPII.

#### References

- [1] Havlik T. Hydrometallurgy 2001. https://doi.org/10.1016/ S0304-386X(01)00178-5.
- [2] Xu H, Wei C, Li C, Fan G, Deng Z, Zhou X, Qiu S. Leaching of a complex sulfidic, silicate-containing zinc ore in sulfuric acid solution under oxygen pressure. Sep. Purif. Technol. 2012;85:206–12. https://doi.org/10.1016/j.seppur.2011.10.012.
- [3] Bulatovic SM. Handbook of flotation reagents: chemistry, theory and practice flotation of sulfide ores 2007. https://doi.org/10.1016/B978-0-444-53029-5.X5009-6.
- [4] Ejtemaei M, Gharabaghi M, Irannajad M. A review of zinc oxide mineral beneficiation using flotation method. Adv. Colloid Interface Sci. 2014;206:68–78. https://doi.org/10.1016/ i.cis.2013.02.003.
- [5] Önal G, Bulut G, Gül A, Kangal O, Perek KT, Arslan F. Flotation of Aladağ oxide lead-zinc ores. Miner. Eng. 2005;18: 279–82. https://doi.org/10.1016/j.mineng.2004.10.018.
- [6] Edraki M, Baumgartl T, Manlapig E, Bradshaw D, Franks DM, Moran CJ. Designing mine tailings for better environmental, social and economic outcomes: a review of alternative approaches. J. Clean. Prod. 2014;84:411–20. https://doi.org/10.1016/j.jclepro.2014.04.079.
- [7] Abkhoshk E, Jorjani É, Al-Harahsheh MS, Rashchi F, Naazeri M. Review of the hydrometallurgical processing of non-sulfide zinc ores. Hydrometallurgy 2014;149:153–67. https://doi.org/10.1016/j.hydromet.2014.08.001.
- [8] Chen T, Yan ZA, Xu D, Wang M, Huang J, Yan B, Xiao X, Ning X. Current situation and forecast of environmental risks of a typical lead-zinc sulfide tailings impoundment based on its geochemical characteristics. J. Environ. Sci. (China) 2020;93:120–8. https://doi.org/10.1016/j.jes.2020.03. 010.
- [9] Xu H, Wei C, Li C, Fan G, Deng Z, Li M, Li X. Sulfuric acid leaching of zinc silicate ore under pressure. Hydrometallurgy 2010;105:186–90. https://doi.org/10.1016/j.hydromet. 2010.07.014.
- [10] U.S.G. Survey. Mineral Commodity Summaries 2024. 2024. p. 2023–4.
- [11] Production D, American N. Mineral Commodity Summaries2023; 2023. p. 2022–3.
- [12] Lottermoser BG. Mine Wastes Characterization, Treatment and Environmental Impacts. Heidelberg: Springer Berlin; 2007. https://doi.org/10.1007/978-3-540-48630-5.
- [13] Reuter MA, Hudson C, Hagelüken C, Heiskanen K, van Schaik A. Metal recycling: opportunities, limits, infrastructure. Nairobi: United Nations Environment Programme; 2013. https://wedocs.unep.org/20.500.11822/8423.
- [14] UN. General Assembly (42nd sess.: 1987-1988). Report of the world commission on environment and development: resolution/adopted by the general assembly. Resolut. Decis. Adopt. by Gen. Assem. Dur. Its 42nd Sess 1987:154–6.
- [15] Asadi T, Azizi A, Lee JC, Jahani M. Leaching of zinc from a lead-zinc flotation tailing sample using ferric sulphate and sulfuric acid media. J. Environ. Chem. Eng. 2017;5:4769—75. https://doi.org/10.1016/j.jece.2017.09.005.
- [16] Li C, Wen Q, Hong M, Liang Z, Zhuang Z, Yu Y. Heavy metals leaching in bricks made from lead and zinc mine tailings with varied chemical components. Constr. Build. Mater. 2017;134:443–51. https://doi.org/10.1016/j.conbuildmat.2016.12.076.
- [17] Chojnacka K, Gorazda K, Witek-Krowiak A, Moustakas K. Recovery of fertilizer nutrients from materials - contradictions, mistakes and future trends. Renew. Sustain. Energy Rev. 2019;110:485–98. https://doi.org/10.1016/j.rser.2019.04. 063.
- [18] Gupta CK. Chemical metallurgy principles and Practice. 2003.
- [19] Jones JBJ. Plant Nutrition and Soil Fertility Manual. Boca Raton, FL: CRC Press - Taylor & Francis Group; 2012.
- [20] Perez JPH, Folens K, Leus K, Vanhaecke F, Van Der Voort P, Du Laing G. Progress in hydrometallurgical technologies to recover critical raw materials and precious metals from low-

- concentrated streams. Resour. Conserv. Recycl. 2019;142: 177–88. https://doi.org/10.1016/j.resconrec.2018.11.029.
- [21] Ayres RU. Metals recycling: economic and environmental implications. Resour. Conserv. Recycl. 1997;21:145–73.
- [22] Mathieux F, Nuss P, Bobba S. Critical raw materials and the circular economy. Luxemburgo: Publications Office of the European Union; 2017. https://doi.org/10.2760/378123.
- [23] Jha MK, Kumar V, Singh RJ. Review of hydrometallurgical recovery of zinc from industrial wastes. Resour. Conserv. Recycl. 2001;33:1–22. https://doi.org/10.1016/S0921-3449(00) 00095-1.
- [24] Monteiro NBR, da Silva EA, Moita Neto JM. Sustainable development goals in mining. J. Clean. Prod. 2019;228: 509–20. https://doi.org/10.1016/j.jclepro.2019.04.332.
- [25] Schulze R, Guinée J, van Oers L, Alvarenga R, Dewulf J, Drielsma J. Abiotic resource use in life cycle impact assessment—Part I- towards a common perspective. Resour. Conserv. Recycl. 2020;154:104596. https://doi.org/10.1016/j. resconrec.2019.104596.
- [26] Vinhal JT, Costa RH, Coleti JL, Espinosa DCR. Iron recovery from zinc mine tailings by magnetic separation followed by carbothermal reduction of self-reducing briquettes. Can. J. Chem. Eng. 2020:1–12. https://doi.org/10.1002/cjce.23845.
- [27] Vinhal JT, Costa RH, Botelho ABJ, Espinosa DCR, Tenório JAS. Gravity separation of zinc mine tailing using Wilfley shaking table to concentrate hematite. In: Miner. Met. Mater. Soc. Springer International Publishing; 2020. p. 1–8. https://doi.org/10.1007/978-3-030-36830-2\_33.
- [28] Vinhal JT, Costa RH, Espinosa DCR, Tenório JAS. Caracterização de rejeito proveniente do processo de flotação do minério willemítico. In: Encontro Nac. Trat. Minérios e Metal. Extrativa. Belo Horizonte, MG.; 2019. p. 1–8.
- [29] Costa RH, Vinhal JT, Espinosa DCR, Tenório JAS. Caracterização do resíduo da flotação do minério de zinco. In: Assoc. Bras. Metal. Mater. e Mineração. São Paulo, SP; 2019. p. 1–10. https://doi.org/10.5151/2594-357X-33193.
- [30] Bale CW, Bélisle E, Chartrand P, Decterov SA, Eriksson G, Gheribi AE, Hack K, Jung I, Kang Y, Melançon J, Pelton AD, Petersen S, Robelin C, Sangster J, Spencer P, Van Ende M. CALPHAD: computer coupling of phase diagrams and thermochemistry FactSage thermochemical software and databases, 2010 2016. Calphad 2016;54:35–53. https://doi.org/10.1016/j.calphad.2016.05.002.
- [31] Bale CW, Bélisle E, Chartrand P, Decterov SA, Eriksson G, Hack K, Jung I, Kang Y. CALPHAD: computer coupling of phase diagrams and thermochemistry FactSage thermochemical software and databases — recent developments. CALPHAD Comput. Coupling Phase Diagrams penalty \z@\protect\futurelet\@let@token Thermochem. 2009; 33:295-311. https://doi.org/10.1016/j.calphad.2008.09.009.
- [32] Paliwal M, Jung I. Calphad Precipitation kinetic model and its applications to Mg alloys. Calphad 2019;64:196–204. https://doi.org/10.1016/j.calphad.2018.12.006.
- [33] Van De Walle A, Nataraj C, Liu Z. Calphad the thermodynamic database database. Calphad 2018;61:173–8. https:// doi.org/10.1016/j.calphad.2018.04.003.
- [34] Ramalingom S, Podder J, Narayana Kalkura S. Crystallization and characterization of orthorhombic β-MgSO4·7H2O. Cryst. Res. Technol. 2001;36:1357–64. https://doi.org/10.1002/1521-4079(200112)36:12<1357::AID-CRAT1357>3.0.CO; 2-7.
- [35] D'Ans J. Phasentheoretisch interessante wafirige Salzsysteme.Die Gewinnung des Rubidiurns aus Carnallit. 1933. p. 3-5.
- [36] Abali Y, Çopur M, Yavuz M. Determination of the optimum conditions for dissolution of magnesite with H2SO4 solutions. Indian J. Chem. Techonology 2006;13:391–7.
- [37] Freyer D, Voigt W. Crystallization and phase stability of CaSO4 and CaSO 4 - based salts. Monatshefte Fur Chemie 2003;134:693-719. https://doi.org/10.1007/s00706-003-0590-3.
- [38] Apelblat A, Korin E. The vapour pressures over saturated aqueous solutions of cadmium chloride, cadmium bromide, cadmium iodide, cadmium nitrate, and cadmium sulphate.

- J. Chem. Thermodyn. 2007;39:1065–70. https://doi.org/10. 1016/j.jct.2006.12.010.
- [39] Aurivillius K. A reinvestigation of the crystal structures of HgSO4 and CdSO4. Zeitschrift Für Krist. - Cryst. Mater. 1980;129:121-9. https://doi.org/10.1524/zkri.1980.153.14.121.
- [40] Lide DR. CRC handbook of chemistry and physics. In: Occup. Environ. Med. 76th edition, 53; 1996. p. 504. https:// doi.org/10.1136/oem.53.7.504.
- [41] Duarte H. Ferro Um elemento químico estratégico que permeia história, economia e sociedade. Quim. Nova 2019; 42:1146-53. https://doi.org/10.21577/0100-4042.20170443.
- [42] Lázaro García A. Nano-silica Production at Low Temperatures from the Dissolution of Olivine. Eindhoven University of Technology; 2014. https://doi.org/10.6100/IR774494
- [43] Dutrizac JE. Calcium sulphate solubilities in simulated zinc processing solutions. Hydrometallurgy 2002;65:109-35. https://doi.org/10.1016/S0304-386X(02)00082-8.
- Shen L, Sippola H, Li X, Lindberg D, Taskinen P. Thermodynamic modeling of calcium sulfate hydrates in the CaSO4-H2O system from 273.15 to 473.15 K with extension to 548.15 K. J. Chem. Eng. Data 2019;64:2697-709. https://doi.org/10. 1021/acs.jced.9b00112.
- [45] Williams ML, CRC handbook of chemistry and physics. In: Occup. Environ. Med.. 76th edition, 53; 1996. https://doi.org/ 10.1136/oem.53.7.504. 504-504.
- [46] Puthiya S, Mucci A, Arakaki T. Dolomite dissolution in aqueous solutions in the presence of nucleotides and their structural components at 25°C and pCO 2 ~ 1 atm Dolomite dissolution in aqueous solutions in the presence of nucleotides and their structural components at 25°C and pCO. Chem. Geol. 2017;465:64-74. https://doi.org/10.1016/j.chemeo.2017.05.022
- [47] Tolonen ET, Rämö J, Lassi U. The effect of magnesium on partial sulphate removal from mine water as gypsum. J. Environ. Manage. 2015;159:143-6. https://doi.org/10.1016/j. jenvman.2015.05.009.
- [48] Ku Y, Wu MH, Shen YS. A study on the cadmium removal from aqueous solutions by zinc cementation. Sep. Sci. 2002;37:571-90. https://doi.org/10.1081/SS-Technol. 120001448.
- [49] Sadegh Safarzadeh M, Bafghi MS, Moradkhani D, Ojaghi Ilkhchi M. A review on hydrometallurgical extraction and recovery of cadmium from various resources. Miner. Eng. 2007;20:211-20. https://doi.org/10.1016/j.mineng.2006.07.001.
- [50] Younesi SR, Alimadadi H, Alamdari EK, Marashi SPH. Kinetic mechanisms of cementation of cadmium ions by zinc powder from sulphate solutions. Hydrometallurgy 2006;84: 155–64. https://doi.org/10.1016/j.hydromet.2006.05.005.
- [51] Wanderley K, Botelho Junior AB, Espinosa DCR, Tenório JAS. Kinetic and thermodynamic study of

- magnesium obtaining as sulfate monohydrate from nickel laterite leach waste by crystallization rio. J. Clean. Prod. 2020; 272:1-13. https://doi.org/10.1016/j.jclepro.2020.122735.
- [52] Shi-bao C, Meng W, Shan-shan LI, Zhong-qiu Z. Overview on current criteria for heavy metals and its hint for the revision of soil environmental quality standards in China. J. Integr. Agric. 2018;17:765-74. https://doi.org/10.1016/S2095-3119(17)61892-6.
- [53] CONAMA. Resolução No 420, De 28 De Dezembro De 2009, Diário of. Da União Nº 249 2013. 2009. p. 81-4. https://doi. org/10.1017/CBO9781107415324.004.
- Asuquo E, Martin A, Nzerem P, Siperstein F, Fan X. Adsorption of Cd (II) and Pb (II) ions from aqueous solutions using mesoporous activated carbon adsorbent: equilibrium, kinetics and characterisation studies. Biochem. Pharmacol. 2017;5:679-98. https://doi.org/10.1016/j.jece.2016.12.043.
- [55] Li B, Wang X, Wei Y, Wang H, Barati M. Extraction of copper from copper and cadmium residues of zinc hydrometallurgy by oxidation acid leaching and cyclone electrowinning. Miner. Eng. 2018;128:247–53. https://doi.org/10.1016/j. mineng.2018.09.007.
- [56] Zárate-Gutiérrez R, Lapidus GT. Anglesite (PbSO4) leaching in citrate solutions. Hydrometallurgy 2014;144-145:124-8. https://doi.org/10.1016/j.hydromet.2014.02.003.
- Chen L, Liao G, Qian Z, Chen J. Vibrating high gradient magnetic separation for purification of iron impurities under dry condition. Int. J. Miner. Process. 2012;102-103:136-40. https://doi.org/10.1016/j.minpro.2011.11.012.
- [58] Fuerstenau MC, Han KN. Principles of Mineral Processing.
- Society for Mining, Metallurgy, and Exploration, Inc.; 2003. [59] Yeh HW, Tang YH, Chen PY. Electrochemical study and extraction of Pb metal from Pb oxides and Pb sulfate using hydrophobic Brønsted acidic amide-type ionic liquid: a feasibility demonstration. J. Electroanal. Chem. 2018;811: 68-77. https://doi.org/10.1016/j.jelechem.2018.01.031.
- [60] Andrews D, Raychaudhuri A, Frias C. Environmentally sound technologies for recycling secondary lead. J. Power 2000;88:124-9. https://doi.org/10.1016/S0378-Sources 7753(99)00520-0.
- [61] Pan D, Li L, Tian X, Wu Y, Cheng N, Yu H. A review on lead slag generation, characteristics, and utilization. Resour. Conserv. Recycl. 2019;146:140–55. https://doi.org/10.1016/j. resconrec.2019.03.036.
- [62] Bechir JLC, Baptista JR, de AD, Souza, Martins E. Determination of maximum zinc recovery of Vazante mine ore by flotation process. REM - Int. Eng. J. 2019;72:315-20. https:// doi.org/10.1590/0370-44672018720069.
- [63] Bechir JLC. Avaliação do impacto da granulometria e da liberação na flotação do minério de zinco da mina de Vazante. 2019.